Contrib Mineral Petrol (1985) 89:239–255

Contributions to Mineralogy and Petrology

Petrology and origin of primitive lavas from the Troodos ophiolite, Cyprus

W.E. Cameron
Department of Geology, Australian National University, G.P.O. Box 4, Canberra A.C.T. 2601, Australia

Abstract. Parental magmas to the Troodos ophiolite are characterised by low TiO_2 and Al_2O_3 and high SiO_2. Extremely fresh and chemically primitive (high MgO) rocks are found within the Upper Pillow Lavas and along the Arakapas Fault Belt of Cyprus and contain forsteritic olivine ± enstatite and groundmass clinopyroxene set in glass or plagioclase, with accessory magnesiochromite and sometimes hornblende. They are quartz-normative and may have originally contained up to 3 wt% H_2O. Geochemically, there are three distinct groups of primitive lavas, based on TiO_2 and Zr contents but also reflected by CaO, Na_2O and REE abundances. These groups cannot be related by crystal fractionation and are considered to have been generated by incremental melting of a variably depleted source region. The parental magma to the least depleted group (Group I) was that of the major portion of the Troodos plutonic complex and is similar to those postulated for other "low-Ti" ophiolites. Chemically it has close affinities with komatiitic basalts. The most depleted lavas (Group III) all have U-shaped REE profiles and variable $^{143}Nd/^{144}Nd$ ratios, interpreted in terms of metasomatism of the source region by an incompatible element-enriched component which was probably derived from a subducted slab. These lavas represent an intermediate step in the development of boninite series rocks.

Introduction

Although the Troodos occurrence is generally considered to be the most thoroughly investigated example of an ophiolite association (Coleman 1977), its petrological affinity and tectonic setting are by no means clear. Primitive (Mg-rich) rocks analogous to those of the Upper Pillow Lava (UPL) group and from the Arakapas Fault Belt (AFB), Cyprus, have not yet been recovered on deep-sea drilling and dredging programs. The Lower Pillow Lavas (LPL) are thought to represent back-arc basin crust and the UPL a different suite with island-arc affinities (Pearce 1975; review by Robinson et al. 1983).

Three lines of evidence have since emerged which have changed the status of the UPL and AFB lavas from off-axis curiosities to potential parental magmas for "low-Ti" ophiolites (Serri 1981; Jaques et al. 1983), of which Troodos is a prime example. These are: the recognition of units within the LPL sequence which have identical textures and chemistry to primitive UPL (Desmet 1976), melting models based on rare-earth element (REE) abundances which relate the UPL and LPL petrogenetically (Smewing and Potts 1976; Wood 1979) and mineralogical studies, particularly of spinels, which demonstrate that the phenocryst and microphenocryst compositions in the UPL and AFB lavas are similar to those found in the lower portion of the Troodos cumulate sequence (Cameron et al. 1980). Robinson et al. (1983) showed that fresh glasses from differentiated LPL and UPL lie on smooth chemical trends. In this project relatively more magnesian rocks (>8% MgO) were investigated in the hope of revealing the chemical characteristics of the source region(s), its melting history and the relationship of the primitive lavas to the suite described by Robinson et al. (1983). From previous comparative studies I had concluded that the most primitive Cyprus rocks constituted the low-SiO_2 end member to the boninite "series" (Cameron et al. 1979, 1980, 1983); this paper elaborates on that theme.

Geological setting

The UPL form a narrow discontinuous belt around the Troodos Massif and serpentinite of the Limassol Forest to the south. They are also found extensively in the Akamas Peninsula and in narrow thrust slices bounded by serpentinite in the Mamonia area (Fig. 1). In tectonically undisturbed regions they have a stratigraphic thickness of up to 500 m and are separated from the underlying LPL by a metamorphic discontinuity (based on zeolite mineralogy: Gass and Smewing 1973) or, in places, a stratigraphic unconformity (Smewing et al. 1975). Robinson et al. (1983) distinguished three petrologic units in the lava sequence 5 to 25 km west of Margi, an 800–1000 m thick basal and middle sequence constituting the LPL in the older terminology and an upper sequence 100–300 m thick approximately equivalent to the UPL.

Between the peridotites of the Limassol Forest and the main Troodos massif lies the AFB, a linear present-day topographic depression extending E-W for 35 km. Simonian and Gass (1978) distinguished two lava successions, a lower one, or Axis Sequence, erupted onto a brecciated basement of sheeted dyke complex and containing intercalated sediments, unconformably overlain by a sequence of lower metamorphic grade which they termed UPL. This distinction has been retained in Fig. 1 but because of the

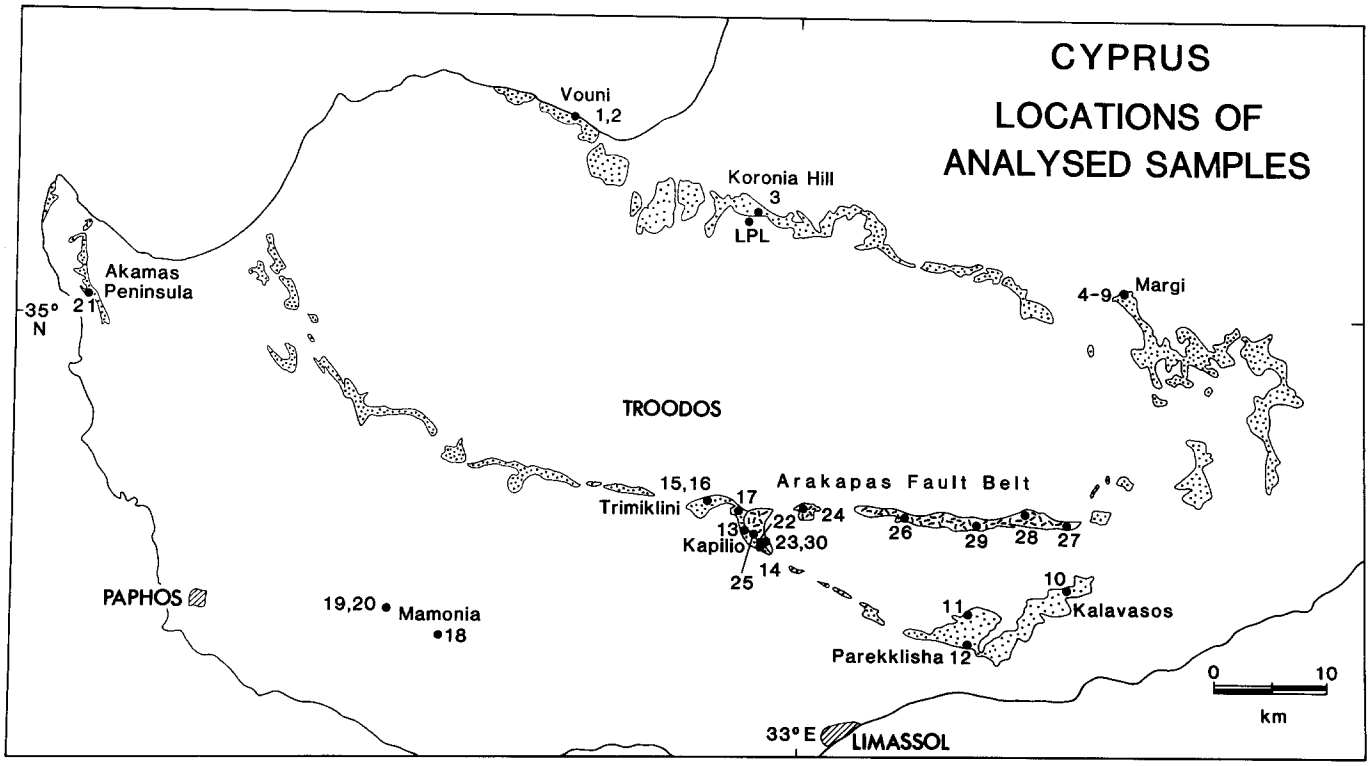

Fig. 1. Locations of analysed samples. 1–21: Upper Pillow lavas (*dotted*), 22–30: Arakapas Fault Belt lavas (*stippled*). Outcrop from Pantazis (1969), Lapierre (1972) and Simonian and Gass (1978)

striking similarities between their lower sequence and the UPL (rather than the LPL of the main massif, Cameron et al. 1980) the term AFB lavas is used here as the exact equivalent of Simonian and Gass' Axis Sequence.

Much of the outcrop of UPL and AFB lavas consists of highly weathered material in which pillow outlines can be distinguished but calcite, zeolites, limonite and smectites have replaced much of the original rock. Feldspar alters readily and thus enables a distinction to be made in the field between the primitive, feldspar-free black pillows (the "limburgites" of Bear 1960), deep green pillows with glassy feldspar-free margins and cores with plagioclase microlites and the more differentiated grey, feldspar-bearing varieties. The crystallisation of plagioclase is, of course, controlled by cooling rate, but its non-appearance in primitive pillows must be related to their chemistry. The sampling strategy was to find the least altered rocks and to that end, pillows with calcite veins or carbonate pseudomorphs after olivine were avoided, as were those with obvious zeolite replacements and infillings. In some areas, hydrothermal alteration is extremely patchy, allowing the eventual collection of reasonably fresh material, but in other areas, pervasive alteration covers many km^2. Large tracts of outcrop were also unsampled because of political difficulties in Cyprus and time constraints.

Pillows are a fairly uniform size, commonly $0.8 \times 0.7 \times 0.5$ m, but sometimes very much smaller. The least altered primitive lavas are readily distinguished by the black glassy nature of the pillow surfaces. The cores of these pillows are greyer but often still relatively unaltered and several core-margin pairs were collected to assess the effects of element mobility during alteration and/or crystal settling. More altered pillows have bluish-purple glassy margins usually about 5 cm wide and completely altered interiors. In these margins, olivine may still be fresh between brown circular patches of smectite spaced in the order of 1 cm apart and up to 2 mm in diameter. Plagioclase phenocrysts were not seen in any pillows. A few contain olivine phenocrysts over 1 cm in length but in these pillows, no vertical zonation was seen. Green to black orthopyroxene phenocrysts are present in possibly 10% of pillows always occurring with olivine or its alteration products.

Samples

The thirty rocks chosen for analysis from the 155 collected in the field are a compromise between petrographic type, freshness and geographic location. They are numbered according to location (Fig. 1): 1–21 clockwise around the massif and 22–30 within the lower or AFB lavas of Simonian and Gass (1978). A single sample of fresh LPL (205) was also analysed, to highlight the isotopic and chemical differences between the LPL and UPL.

Beginning with the UPL, the cliff at Vouni consists of relatively unaltered orthopyroxene phyric pillow lavas. East of Koronia Hill, fresh purplish selvages to pillows may be found. The least altered of the material collected there was sample 29473 figured in Cameron et al. (1979).

The Margi area (Gass 1958) contains four different rock types: samples 4–6 are glassy pillows from excellent exposures along the Alikos River, no. 7 is from a plagioclase-bearing flow, sample 8 a holocrystalline picritic dyke forming a prominent "peridotite" hill (Gass 1958) and sample 9, portion of an "ultrabasic" pillow lava nearby.

The Kalavasos area contains abundant fresh pillows (sample 10) which unconformably overlie mineralised LPL (Adamides 1980). In much of the rest of the island, the more primitive members tend to be stratigraphically higher. The "picrite-basalts" of Searle and Vokes (1969) north of the Vasilikos River were not analysed because of their inhomogeneously distributed olivine phenocrysts. Olivines in sample 10 are very much smaller, about 0.5 mm across.

The extensive outcrop of pillow lavas north of Parekklisha contains two primitive types, orthopyroxene-phyric (sample 11, collected from 3.5 km N of the village close to the area mapped as LPL by Pantazis 1967) and much of the rest, almost aphyric (sample 12).

One of the best exposures in Cyprus of very fresh primitive rocks occurs near Kapilio at the western end of the AFB. Samples 13 and 14 were collected from the UPL near the boundary with the stratigrapically lower AFB sequence (Simonian and Gass 1978) and samples 22, 23, 25 and 30 within it. It is not known whether sample 103A of Kay and Senechal (1976) which is reanalysed here comes from the UPL or AFB in this area. Samples 15 and 16 are the margin and core respectively of a very fresh glassy pillow and sample 17 a glassy rind 5 cm thick to a pillow with an altered core.

The Mamonia Complex is composed of an assemblage of Upper Triassic to Lower Cretaceous sedimentary rocks and Upper Triassic metabasalts of alkaline affinity (Lapierre and Rocci 1976). A study of igneous rocks in the thrust sheets forming an arcuate belt through the SW part of the Complex was suggested to the author by A.H.F. Robertson and this confirmed the presence of a substantial proportion of pillows with Troodos UPL-like textures. Sample 18 comes from the easternmost thrust sheet 2.5 km due E of Phasoula and samples 19 and 20, margin and core respectively of the same pillow from an extensive outcrop 1–2 km NW of Phasuola (Swarbrick 1980). The UPL of the Akamas Peninsula have been overthrust by serpentinised harzburgite and are probably themselves part of a thick semi-horizontal thrust sheet. Sample 21 was the least altered and is a grey pillow core. Orthopyroxene-free lavas are not as common and are more altered.

In the Arakapas Fault Belt, primitive lavas make up about 30% of the pillow outcrop (Simonian and Gass 1978), perhaps 10% greater than for the UPL, although it is very difficult to make quantitative estimates because of alteration. Samples 24 and 26–29 are five of 32 collected along the main part of the belt.

Petrography, mineral chemistry and alteration

Primary igneous textures

Most of the primitive UPL and AFB pillow lavas analysed in this study are olivine- or olivine-orthopyroxene vitrophyres. Olivine occurs commonly as microphenocrysts, sometimes accompanied by orthopyroxene and rarely by clinopyroxene. All three can occur as equant groundmass crystals and/or with skeletal morphologies, set in a colourless, yellow or brown glass. Typical modes are given in Cameron et al. (1983) for samples 2, 15 and 28, numbers 8–10 respectively of that study. Euhedral magnesiochromite is a ubiquitous accessory. In about a quarter of the samples sectioned, pale green amphibole has developed as overgrowths on skeletal augite or as tiny rosettes in glass. Plagioclase is found in the cores of some pillows of primitive lavas (e.g. sample 21), subhedral and hopper crystals in dykes (sample 8) and, generally, in more differentiated UPL (e.g. sample 7) with intersertal textures. The order of crystallisation in the UPL and AFB rocks is:

$$\text{chr} - \text{ol} - \text{opx} - \text{cpx} - \text{plag} \quad (1)$$

$$\text{or} \quad \text{chr} - \text{ol} - \text{cpx} - \text{opx} - \text{plag} \quad (2)$$

The second was considered to be the order of crystallisation in the plutonic complex by Greenbaum (1972).

The texture of a given specimen depends on its degree of supercooling. Hyaloclasites and tachylitic margins to pillows usually contain sporadic olivine microphenocrysts, sometimes with minute spinel inclusions, set in glass. Close to pillow margins, textures are as in Fig. 2a: olivine is of microphenocryst size and the pyroxene is acicular, sometimes with a 'cockscomb' appearance of curved, branching dendrites. In the core of most primitive pillows, clinopyroxene is even more strongly acicular and olivines slightly larger. The latter also may appear in the groundmass as highly skeletal forms. There are two textural variants which probably owe their origin to chemical factors as well as degree of supercooling. Olivine microphenocrysts often have hopper morphologies similar to those depicted in Donaldson's (1976) Fig. 1B or Fig. 8 with experimentally determined cooling rates of 2.5°/hr. They could easily be mistaken for resorbtion characteristics but occasionally display the "lantern" {021} form and therefore result from crystal growth. Such rocks, for example sample 3 (Fig. 1a of Cameron et al. 1979; Fig. 3c of Cameron et al. 1980) have acicular clinopyroxene but not of skeletal form. The other variant was found only in pillows of the Margi area: equant olivines with lantern and harpoon morphologies of microphenocryst size e.g. sample 6 (Fig. 2b; see also Fig. 3.2 h of Cameron and Nisbet 1982). These suggest a possible cooling rate of 7–15°/hr and occur with acicular skeletal augite and groundmass "chain" olivine with a suggested cooling rate of 80°/hr.

Vesicles are not abundant and are usually confined to the narrow peripheral zone of pillows. Where they occur, they are relatively small and filled with secondary minerals and thus avoided as far as possible for analytical purposes. In a number of rocks, however, there are spherical glassy segregations up to 2 mm across, sometimes with an amygdale (Fig. 2c). Where amphibole is present, it is usually more abundant and much coarser-grained in the segregation (c.f. Cape Vogel boninites: Walker and Cameron 1982).

Mineralogy

Olivine occurs as five morphological types: xenocrysts, phenocrysts, microphenocrysts, equant groundmass grains and highly skeletal, late crystallising forms. Microphenocrysts are between 0.6 and 0.1 mm across, phenocrysts larger (usually >1 mm) and groundmass grains smaller. The large (up to 10 mm) olivines in the 'ultrabasic' pillow lavas (e.g. sample 9) are mainly euhedral but have occasional embayments, interpreted as resorption features. In addition, 5–10% display kink-bands. These have compositions between $Fo_{91.3}$ and $Fo_{92.6}$ (Table 1), slightly more magnesian than in any of the other rock types and are probably xenocrysts. Euhedral olivines of similar size but without kink-bands are found in the "Type 4" picritic dykes of Desmet et al. (1978). These are phenocrysts and range in composition from $Fo_{90.2}-Fo_{91.5}$. Olivines in a less primitive picritic dyke (sample 8) are 2–4 mm long and uniformly Fo_{89}. Other samples which have obvious olivine phenocrysts are nos. 7 and 25–28. In no. 7 they make up 10% but in others $<5\%$ of the mode and therefore would not be expected to have a significant effect on bulk rock chemistry. In sample 26, the olivines are $Fo_{90.5}$ and no. 28, Fo_{88-89}.

Near-euhedral olivine microphenocrysts vary from $Fo_{90-90.5}$ in samples 13–16 to $Fo_{86.5}$ in sample 1. The highly skeletal grains in samples 4 and 6 are zoned, from Fo_{89} to Fo_{87} at delicate quench margins. "Groundmass" olivine in all samples is usually 1–4 mol % less magnesian. Equant olivine in sample 3 is Fo_{83} (Table 1), tiny swallow tail olivines in the ultramafic lava (sample 9) Fo_{87-89} and chain olivine in samples 6 and 23, Fo_{85} and Fo_{86} respectively. Cr_2O_3 contents are <0.04 wt% (Cameron and Nisbet 1982), below the detection limit for the microprobe used in this study.

It is a reasonable assumption that groundmass olivine and skeletal microphenocrysts crystallised *in situ*. The phenocrysts probably crystallised in a high level magma chamber. Euhedral

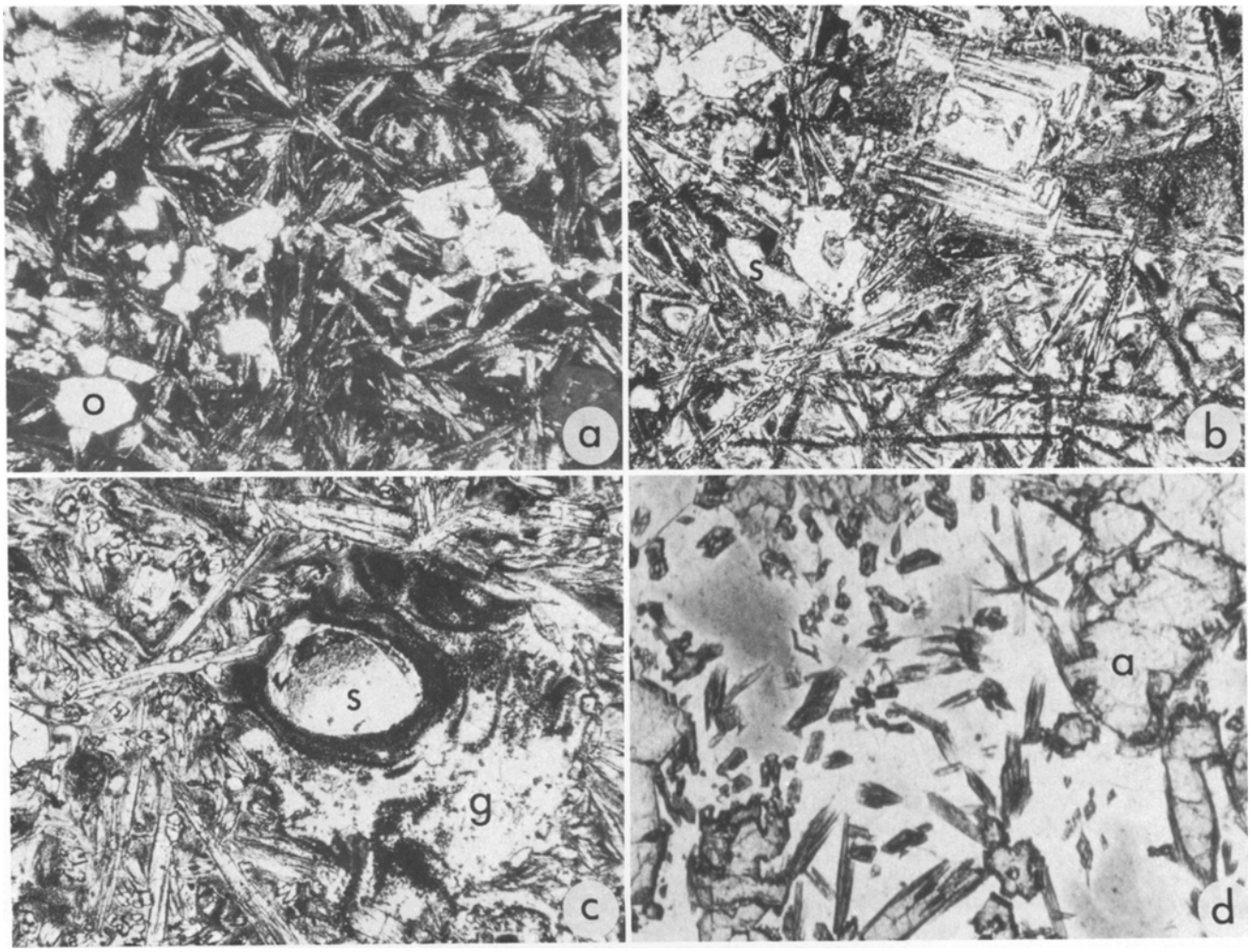

Fig. 2a–d. Textural features of primitive Troodos lavas. **a** Typical pillow margin, 1–2 cm from the glassy selvage. Sample 15, equant olivine microphenocrysts (O, $Fo_{90-90.5}$ with occasional skeletal morphology and acicular augite with feathery terminations set in glass (dark). Crossed polars. Width of field 2.0 mm. **b** Margin of pillow lava, Margi area, showing three types of olivine morphology: hopper (*left side*), lantern (*top, centre*), both Fo_{87-89}, and chain (dark acicular grains clearly visible in lower part of photograph), Fo_{85}. Smectite (s) partly replaces glass. Sample 6, PPL. Width of field 2.0 mm. **c** Volatile-rich segregation, sample 3. Vesicle is filled by smectite (*s*) and surrounded by a pyroxene-free glassy region (*g*) from which tiny quench amphiboles (*dark patches and trains*) have crystallised. PPL. Width of field 2.0 mm. Compare Fig. 1c of Cape Vogel boninite (Walker and Cameron 1983). **d** Late-crystallising ferrohornblende, sample 22, as overgrowths on augite (a) and independent, sometimes skeletal crystals in glass. PPL. Width of field 1.5 mm

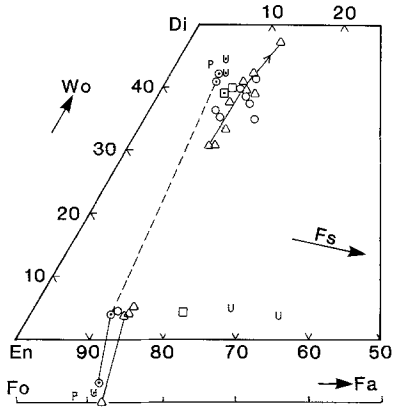

Fig. 3. Representative pyroxene compositions and their coexisting olivines Symbols: □, sample 7; △, sample 3; ○, sample 28 U, sample 8; P, large (10–15 mm long) phenocrysts in picrite dyke 1 km S. of Kionia. Dots in centres of symbols characterise more normal sized phenocrysts; arrow shows typical compositional trend of groundmass augites with increasingly skeletal morphologies

Table 1. Representative microprobe analyses of olivine

Sample	9	15	3	
	xenocryst	micro-phenocryst	micro-phenocryst	ground-mass
SiO_2	40.98	40.71	40.42	40.14
FeO*	8.18	9.59	11.17	15.90
MnO	0.10	0.15	0.16	0.20
MgO	49.74	48.96	47.42	43.24
CaO	0.20	0.23	0.30	0.35
NiO	0.31	0.41	0.33	0.23
Total	99.51	100.05	99.80	100.06
$\frac{100\,Mg}{Mg+Fe^{2+}}$	91.6	90.1	88.3	82.9

FeO*: total iron reported as FeO

Table 2. Representative microprobe analyses of orthopyroxene

Sample	28 phenocryst	3	24 groundmass	22
SiO_2	56.43	55.95	55.06	52.03
Al_2O_3	0.59	1.40	2.39	4.93
FeO*	7.50	7.56	8.96	13.52
MnO	0.07	0.22	0.28	0.15
MgO	32.13	31.29	29.74	26.82
CaO	2.20	2.08	2.74	1.99
Cr_2O_3	0.41	0.71	0.68	n.d.
Total	99.33	99.21	99.85	99.44
$\frac{100\,Mg}{Mg+Fe^{2+}}$	88.6	88.0	85.5	80.3

Table 3. Representative microprobe analyses of clinopyroxenes

Sample	P phenocryst	28 microphenocryst	3 groundmass		
SiO_2	54.22	53.78	52.59	51.30	48.76
TiO_2	nd	nd	0.25	0.39	0.51
Al_2O_3	1.31	1.44	3.49	5.02	8.29
FeO*	3.03	4.14	7.07	7.27	7.75
MnO	nd	nd	0.24	0.16	0.16
MgO	18.74	18.45	19.71	16.93	13.02
CaO	22.06	21.23	16.41	19.05	21.66
Cr_2O_3	0.43	0.90	0.33	0.15	nd
Total	99.79	99.94	100.09	100.27	100.15
En	51.6	51.2	55.9	49.0	39.6
Wo	43.7	42.4	33.4	39.7	47.4
Fs	4.7	6.4	10.7	11.3	13.0

nd = not detected
Sample P is a picritic dyke, 1 km S. of Kionia

microphenocrysts, e.g. many of those in Figs. 2a, b, probably crystallised just prior to eruption from the liquid which ultimately formed the pillow lavas. Only crystals >1 mm show any tendency to settle within individual pillows. Samples 2 and 7–9 are the only ones exhibiting accumulation of phenocrysts (in the first case orthopyroxene and for the others, olivine) and therefore are not "liquid" compositions.

Orthopyroxene occurs as euhedral phenocrysts or microphenocrysts in six of the analysed rocks and in the groundmass of nine others. Orthopyroxene-bearing lavas are not restricted to a particular location but, notably, are not found in the primitive Margi pillow lavas. It does appear, however, as a late-crystallising phase in plagioclase-bearing lavas and dykes from that area (samples 7, 8).

Orthopyroxene phenocrysts form isolated crystals or occasionally clots (Fig. 3.3a in Cameron and Nisbet 1982). They are not spatially related to olivine in any way and show no sign of having been in a reaction relationship with olivine. Their compositions are remarkably uniform, En_{88-89} (Table 2), whereas those of microphenocryst and groundmass orthopyroxene jacketed by clinopyroxene such as those in sample 3 (centre of Fig. 1a in Cameron et al. 1979) vary between En_{86} and En_{88}. In rocks where clinopyroxene (endiopside) has crystallised after olivine, orthopyroxene appears rimming clinopyroxene or as small, elongate prisms in the groundmass (sample 22) or as individual groundmass crystals (samples 7 and 8). In these cases, the pyroxene is much more Fe-rich (En_{65-80}) than even tiny groundmass prisms in rocks with the order of crystallisation olivine → orthopyroxene → clinopyroxene (Table 2, Fig. 3). The alumina contents of the orthopyroxene phenocrysts are <0.8 wt% Al_2O_3 and often less than 0.4%, suggesting a low-pressure origin. Prisms of groundmass orthopyroxene rimmed by augite (samples 3, 24; Table 2) have Al_2O_3 contents up to 3 wt% reflecting rapid crystallisation. Overgrowths on augite are also highly aluminous (sample 22, Table 2). The very low-Ca pyroxene, clinoenstatite, was not found and would not be expected to crystallise.

Clinopyroxene occurs as occasional phenocrysts up to 15 mm long in picritic dykes, e.g. sample 8 and those in the area described by Desmet et al. (1978). None of the analysed pillow lavas contain clinopyroxene phenocrysts, but they were present in a few altered samples. The majority of primitive lavas crystallise Ca-rich pyroxene after olivine and this appears as microphenocrysts (samples 5, 13 and 27), more commonly as an equant groundmass phase, and is ubiquitous in lavas as acicular, often skeletal grains, forming a hyalopilitic texture. The most spectacular forms are dendrites sometimes 0.05 × 2 mm with three dimensional morphologies identical to those described by Fleet (1975) from a komatiitic basalt.

Representative clinopyroxene compositions from the three geochemical groups (defined later) and a picrite dyke are shown in Fig. 3 with tielines drawn between inferred near-equilibrium compositions in sample 28. Phenocrysts and microphenocrysts are endiopsides (Table 3, Fig. 3) whereas groundmass clinopyroxene is more Fe-rich, and typically augite. Equant groundmass clinopyroxene in rocks which crystallise orthopyroxene first (e.g. no. 3) is commonly relatively low in Wo component, but with increasingly skeletal morphologies, they approach the Di–Hd join (arrowed curve, Fig. 3). This is accompanied by increased Al_2O_3, TiO_2 and a drop in Mg/Fe ratio and Cr content.

The presence of magnesian pigeonite is suspected in some rocks (Cameron et al. 1979; 1980). Electron-probe analyses similar to those reported by Arndt and Fleet (1979) in komatiites were obtained in narrow zones between orthopyroxene and augute in four samples, but these may represent analyses straddling low-angle orthopyroxene-augite grain boundaries. More detailed crystallographic studies will have to be carried out before the existence of magnesian pigeonite can be considered proved.

Hornblende with a pleochroic scheme α = pale yellow, β = green, γ = bluish green was coarse-grained enough to analyse in sample 22. It occurs as overgrowths on augite, orthopyroxene and as individual acicular grains up to 0.2 mm long or small rosettes in glass (Fig. 2d). In most rocks where amphibole could be recognised, the crystals were much smaller, for example in Fig. 5b of Cameron et al. (1980), a photomicrograph of sample 9 whose caption appeared inadvertently as Fig. 5c in that paper. The amphibole is a ferro-hornblende with $Mg/(Mg+\Sigma Fe)=0.48$ (Table 4), and is inferred to be of primary igneous origin.

Plagioclase occurs in the groundmass of samples 7, 8 and 15. In sample 7, it is An_{78} and in picrite dykes, An_{70-84}. Gass (1958) reported plagioclases as calcic as An_{95} in a similar rock but these were not found in the course of this study.

Spinel in all rocks is a deep red magnesiochromite which occurs in lavas either as inclusions in olivine or relatively small groundmass euhedra ~0.05 mm across. In samples 7, 9 and picrite dykes larger grains occur, up to what are considered to be phenocryst size, 0.5 mm across. Very few display higher reflectance rims. Chemically, they lie between $Cr/(Cr+Al)=0.68$–0.85 and $Mg/(Mg+Fe^{2+})=0.50$–0.70 when recalculated assuming 24 cations (Table 5, Fig. 4).

The compositional field is similar to that of spinels in the cumulate ultramafic part of the Troodos complex (Cameron et al. 1980; Greenbaum 1977). There is a considerable range in spinel composition within a thin section and the only chemical generalisation that can be made is that phenocrysts are more magnesian than groundmass spinels. In less primitive UPL, magnesiochro-

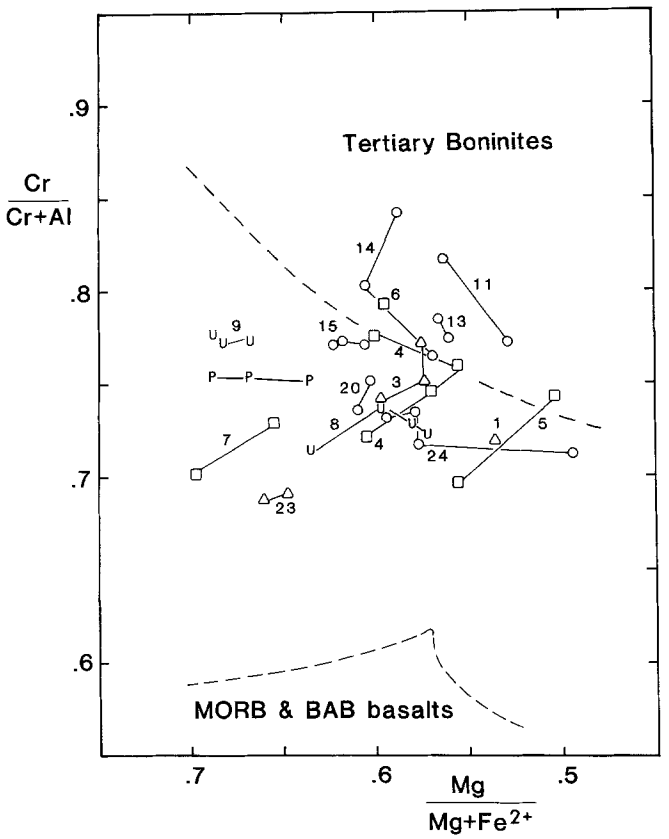

Fig. 4. Magnesiochromite compositions projected onto the base of the spinel prism. Fe^{2+} calculated, assuming stoichiometry. Spinels in the picrite dykes (P, 9) and sample 7 are phenocrysts. Lines join spinels from same sample. Field for spinels in Tertiary boninites from Cameron et al. (1980) and lower bound from Cape Vogel boninites (D.A. Walker, unpublished data). Field for mid-ocean ridge and back-arc basin basalts (MORB, BAB) from Dick and Bullen (1984)

Table 4. Microprobe analysis of quench amphibole

Sample	22	Calc to 23 O	
SiO_2	46.07	Si	6.703
TiO_2	0.52	Al	2.562
Al_2O_3	14.94	Ti	0.057
FeO*	15.42	Fe	1.876
MnO	0.15	Mn	0.018
MgO	7.84	Mg	1.700
CaO	12.81	Ca	1.997
Na_2O	0.24	Na	0.068
K_2O	0.13	K	0.024
Total	98.12		15.005

mites have lower Cr/(Cr + Al) values (Jørgensen and Brooks 1981; Dick and Bullen 1984).

Alteration

The UPL and AFB rocks belong to the zeolite facies of metamorphism (Gass and Smewing 1973) and they have also been extensively metasomatised. The maximum temperature of metamorphism was thought to be below 100° C by Gass and Smewing (1973), consistent with the formation of analcime, low-T zeolites and smectite. Whole rock K_2O contents are often above 1% and may reach 5% and Fe_2O_3/FeO ratios, CO_2 and Na_2O are very variable (Moores and Vine 1971). The present study proves that very fresh material exists (but is not always easy to find). In these samples textural preservation is perfect and only olivine and glass show any degree of alteration. Rocks with adularia, secondary quartz, completely altered glass or more than minimal amounts of calcite or zeolite were not analysed. The extent of alteration has been estimated qualitatively for each analysed sample at the foot of Table 6 where five criteria are documented from 'pristine' (1) to 'altered, but with minimal metasomatism' (4). Category 5 applies only to the LPL sample which has about half its vesicles infilled by silica.

Table 5. Representative microprobe analyses of spinels

Sample	14 g-mass	9 phc	6 g-mass	23 g-mass
TiO_2	0.21	0.29	0.49	0.33
Al_2O_3	7.81	11.23	12.58	15.16
Cr_2O_3	61.52	58.11	52.80	52.03
V_2O_3	0.22	0.13	0.26	0.20
FeO*	17.47	14.76	21.70	17.70
MnO	0.41	0.16	0.43	0.42
MgO	11.85	14.46	12.05	13.84
Total	99.49	99.14	100.22	99.68
$\frac{Cr}{Cr+Al}$	0.84	0.78	0.74	0.70
$\frac{Mg}{Mg+Fe^{2+}}$	0.59	0.69	0.58	0.65
$\frac{Fe^{3+}}{Fe^{3+}+Al+Cr}$	0.04	0.04	0.08	0.06

g-mass = groundmass, phc = phenocryst
Fe^{2+}, Fe^{3+} calculated assuming stoichiometry

Smectite occurs in all lavas as the commonest alteration product, infilling vesicles and replacing olivine and glass. Only in the ultramafic lava (no. 9) and picrite dykes (e.g. no. 8), are the olivines are partly serpentinised, rather than altered to smectite. There are four chemical groups of smectite, based on MgO content. Saponite with 23–25% MgO always replaces olivine. The other three types are yellowish saponite-nontronite mixtures with 16, 10 and about 7% MgO. The last can easily be distinguished because it is colourless and often can be seen forming from the 16% MgO smectite which replaces olivine and the outer lining of vesicles. The 10% MgO smectite replaces glass and is also found in vesicles (e.g. Fig. 2c).

Although olivine is replaced by a smectite with half its MgO content, glass is replaced and voids filled by a higher-MgO smectite, so preserving much of the original Mg content of the rock. The excess Ca liberated from the alteration of glass probably finds its way into vesicles and is fixed as calcite as well as smectite. Gross changes in SiO_2 or Na_2O are not expected, again because of the balance between olivine, glass and smectite compositions. Potassium however is preferentially concentrated in smectite and is probably the most mobile of the major elements.

Geochemistry

Thirty major and trace element analyses, excluding rare-earth elements (REE), of the freshest rocks collected for this study are given in Table 6. Major elements, Sc, V, Cr

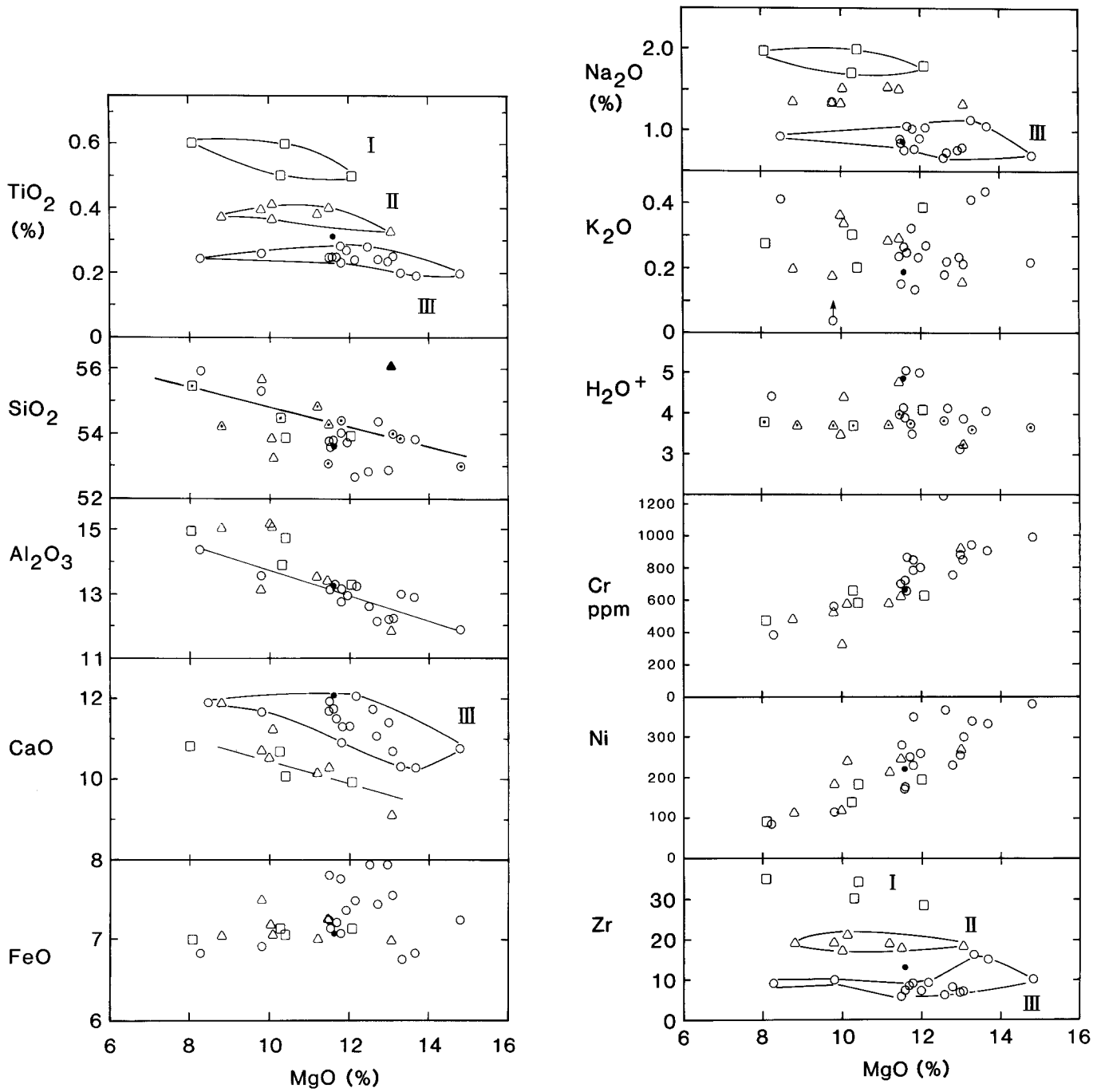

Fig. 5. Major and trace element variation in primitive Troodos lavas with MgO, plotted on a volatile-free basis (except for H_2O^+). Symbols □, △, ○ represent three chemical groupings (I–III respectively). ● = sample 29. Dots in centres of symbols in SiO_2 and H_2O^+ variation define least altered samples (category 1, Table 6). Olivine control lines are shown on SiO_2, Al_2O_3 and CaO plots. FeO normalised to $Fe^{3+}/(Fe^{3+}+Fe^{2+})=0.10$. Solid symbol in SiO_2 variation is sample 2 which contains excess orthopyroxene

and Ba were analysed on a Philips 1450 X-ray fluorescence spectrometer and the remainder on a Philips 1220 instrument. Analyses were by B.W. Chappell, using the method described by Norrish and Chappell (1977). REE, Hf and Pb analyses (Table 7) were by spark-source mass spectrography (SSMS) at the Research School of Earth Sciences, ANU (technique described by Taylor and Gorton 1977).

Major and trace elements, excluding REE

In Fig. 5, major elements (recalculated anhydrous) are plotted against MgO. Magnesium numbers (100 Mg/(Mg+Fe^{2+})) are also given in Table 6 and produce trends similar to those in Fig. 5 when plotted against other major elements. FeO values in Fig. 5 are standardised to $Fe^{3+}/(Fe^{3+}+Fe^{2+})=0.10$, a reasonable ratio since measured values in two minimally altered rocks (nos. 10, 15) are <0.17.

The TiO_2 contents of the UPL and AFB lavas fall into three natural groupings, designated I–III with appropriate symbols in Figs. 3–5 and Table 6. Group III lavas can also be distinguished by higher CaO and lower Na_2O, for given MgO contents. All samples, with the obvious exceptions of nos. 8 and 9 are quartz normative and, on an anhydrous

Table 6. Petrography and chemical composition of primitive rocks from Troodos

	Upper pillow lavas																
	Vouni		Koro-nia	Margi						Kala-vasos	Parekklisha		Kapilio		Trimiklini		
	1	2	3	4	5	6	7	8	9	10	11	12	13	14	15	16	17
SiO_2	52.75	53.80	51.38	52.57	52.04	50.24	51.16	41.85	43.16	51.73	50.52	50.47	51.32	49.81	51.74	50.57	51.37
TiO_2	0.38	0.31	0.36	0.57	0.48	0.46	0.57	0.25	0.16	0.35	0.22	0.23	0.22	0.19	0.19	0.18	0.27
Al_2O_3	12.45	11.40	12.72	14.15	13.29	12.36	13.95	5.12	4.71	14.32	11.19	11.47	12.42	11.22	12.47	12.15	12.12
Fe_2O_3	1.79	1.57	1.82	1.51	2.13	2.20	3.03	4.02	2.57	1.40	2.19	1.66	1.73	2.09	1.20	1.96	1.87
FeO	6.27	6.06	5.63	6.01	5.63	5.37	4.75	4.94	5.40	6.22	5.68	6.35	5.85	5.71	6.10	5.34	6.51
MnO	0.15	0.16	0.15	0.13	0.14	0.14	0.11	0.14	0.13	0.14	0.16	0.14	0.15	0.15	0.14	0.14	0.16
MgO	9.28	12.54	10.51	7.67	9.78	11.20	9.87	31.00	33.70	8.41	11.81	12.25	11.13	13.92	12.74	12.83	11.24
CaO	10.17	8.73	9.50	10.29	10.13	9.20	9.61	2.68	3.63	11.35	10.23	10.00	10.30	10.12	9.88	9.50	10.78
Na_2O	1.30	1.30	1.45	1.88	1.62	1.67	1.91	0.29	0.34	1.27	0.66	0.75	0.97	0.66	1.10	0.99	0.74
K_2O	0.17	0.15	0.27	0.26	0.29	0.35	0.19	0.10	0.10	0.19	0.20	0.20	0.31	0.21	0.39	0.40	0.12
P_2O_5	0.04	0.02	0.04	0.06	0.03	0.05	0.06	0.01	0.00	0.03	0.02	0.02	0.03	0.02	0.01	0.01	0.02
H_2O^+	3.72	3.19	3.78	3.79	3.72	4.04	1.78	6.64	3.56	3.69	4.07	3.85	3.76	3.65	3.60	4.08	3.56
H_2O^-	0.91	0.60	1.93	0.58	0.76	2.01	2.37	2.49	1.35	0.58	2.33	1.44	1.31	1.86	0.56	1.76	0.81
CO_2	0.23	nd	0.22	0.09	nd	0.18	0.11	0.17	0.51	0.14	0.33	0.42	0.10	0.23	nd	nd	0.38
Total	99.61	99.83	99.76	99.56	100.04	99.47	99.47	99.70	99.32	99.82	99.61	99.25	99.60	99.84	100.12	99.91	99.95
Sc	37	37	32	36	38	34	34	15	13	41	40	40	41	40	40	38	43
V	212	194	188	217	211	193	211	86	76	226	219	213	222	212	203	192	226
Cr	520	910	580	470	655	620	570	2,150	2,480	480	750	850	780	980	940	905	850
Ni	183	268	214	83	138	195	183	1,160	1,330	106	230	299	237	378	339	333	352
Rb	4	3	5	6	6	8	4	3	3	4	5	4	7	7	14	12	3
Sr	66	62	96	97	141	135	89	20	25	71	83	73	136	53	62	76	32
Ba	10	12	13	20	20	15	20	15	<5	20	15	15	50	18	45	40	15
Zr	19	18	19	35	30	28	34	15	10	19	8	7	9	10	16	15	9
Nb	<1	1	<1	1	1	<1	1	<0.5	<0.5	1	2	2	<1	<1	1	1	<1
Y	9	9	8	15	13	13	15	6	4	9	7	7	7	7	7	7	9
Mg No.	70.0	76.9	74.1	67.3	72.0	75.1	72.3			69.0	75.3	75.6	74.8	78.4	77.8	78.1	73.1
Q	9.0	7.3	5.6	7.4	5.1	2.4	3.3	–	–	7.0	6.6	5.3	5.9	2.6	3.3	3.2	6.5
Ti/Zr	120	103	114	98	96	99	101	104	102	111	165	197	147	114	71	72	180
Geochemical group	II	II	II	I	I	I	I	I	I	II	III	III	III	III		III	III
Petrography																	
Phenocrysts	o	o					ol	ol	ol		o						
Micro-phenocrysts	o,ol	o,ol	ol	ol*	ol,a	ol*	ol,a	a	ol	ol	o,ol	ol	ol,a	ol	ol*	ol	ol
Groundmass:																	
equant	a,o	a,o	ol,o	ol*	a	ol*	f,a,o	f,a,o	ol*	a	a,o	ol	ol,a,o	ol*,o	ol*	ol*	ol
quench	a	a,am	a,am	a,ol	a	a,ol		a,f	a,am	a	a	a,o	a,am	a,am	a,ol	a,am	a,am
Alteration	1	1	1	1	1	2	4	3	2	1	4	1	1	1	1	2	2

Sample locations as in Fig. 1. Nos. 15 and 16; 19 and 20 are margins and cores respectively of single pillows. Field, petrographic and some chemical data are not available for sample 103A.

Chemical analyses are by XRF (analyst B.W. Chappell) except for Na_2O by flame photometry and H_2O and CO_2 gravimetrically (analysts R.S. Freeman and J. Wasik). The major element analysis of sample 103A was by electron probe on a fused bead and its trace elements by SSMS.

nd=not detected; Mg No.=100 Mg/(Mg/(Mg+Fe^{2+}), with $Fe^{3+}/(Fe^{2+}+Fe^{3+})$ set to 0.10; Q=normative quartz, calculated using this ratio.

Petrographic abbreviations: *ol*=olivine, *o*=orthopyroxene, *a*=augite, *am*=amphibole, *f*=plagioclase feldspar, *q*=quartz. Phases are listed in decreasing order of abundance.

basis, andesitic. The least altered ones (category 1 in Table 6 and specially designated in Fig. 5) *tend* to have higher SiO_2 values and lie on an olivine control line. Olivine control lines have also been drawn for Al_2O_3 in Group III lavas and CaO in Group I and II lavas. There is wide scatter on the K_2O-MgO plot, reflecting alteration, H_2O^+ is almost constant in the freshest samples at 3.2–4.0 wt% whereas H_2O^- varies widely depending on the amount of smectite (or serpentine for samples 8 and 9).

Trace element contents were calibrated against synthetic standards with mass absorption coefficients measured directly. The results (Table 6) are accurate to ±5% for Sc, V and Cr, ±1% for Rb and Sr and ±1 ppm for other, low level trace elements, except for Ba (±2 ppm). Trace

Upper pillow lavas				Arakapas Fault Belt lavas										Lower pillow lava	
Mamonia			Akamas												
18	19	20	21	22	23	24	25	26	27	28	29	30	103A	205	
50.45	49.67	49.51	53.57	52.83	49.54	50.19	49.58	50.54	49.17	49.54	49.01	49.79	52.67	65.80	SiO_2
0.34	0.23	0.23	0.25	0.23	0.38	0.24	0.26	0.37	0.23	0.25	0.28	0.22	0.23	1.07	TiO_2
14.18	12.28	12.18	13.12	13.63	14.00	12.74	11.81	12.50	12.12	11.95	12.15	11.49	13.22	13.47	Al_2O_3
1.84	2.22	2.32	2.58	1.47	2.26	2.19	2.23	1.86	2.58	2.39	2.80	2.70		3.76	Fe_2O_3
5.84	5.37	5.31	5.15	5.82	5.27	6.24	6.27	5.81	5.02	5.41	4.68	5.87	8.30	2.97	FeO
0.15	0.13	0.13	0.12	0.15	0.13	0.15	0.16	0.13	0.16	0.15	0.14	0.15	0.14	0.14	MnO
9.42	10.75	10.65	9.45	7.79	9.41	10.88	11.81	10.69	10.74	11.02	10.62	12.23	12.13	1.27	MgO
9.86	10.96	11.06	11.28	11.27	10.43	11.11	11.03	9.58	10.52	10.45	10.98	10.74	12.07	6.38	CaO
1.26	0.72	0.76	1.33	0.89	1.44	0.83	0.65	1.41	0.94	0.86	0.78	0.74	1.03	2.84	Na_2O
0.35	0.25	0.21	0.03	0.39	0.32	0.14	0.17	0.27	0.23	0.21	0.17	0.22	0.27	0.34	K_2O
0.03	0.02	0.02	0.02	0.01	0.04	0.02	0.03	0.04	0.03	0.02	0.03	0.02		0.09	P_2O_5
3.51	3.93	4.07	1.31	4.24	4.46	4.03	3.85	4.82	5.19	5.04	4.86	3.11		0.91	H_2O^+
2.30	2.75	2.64	1.10	1.44	1.72	1.06	1.70	1.30	2.96	2.27	3.15	2.19		0.65	H_2O^-
nd	0.39	0.36	0.12	nd	0.44	0.24	0.22	0.08	nd	0.14	0.13	0.27		0.03	CO_2
99.53	99.67	99.45	99.43	100.06	99.84	100.06	99.77	99.40	99.89	99.70	99.78	99.74	100.00	99.72	Total
39	42	40	43	46	37	43	40	35	39	41	36	39			Sc
218	226	222	238	248	204	233	219	214	221	220	201	220		226	V
320	630	710	550	390	580	650	1,250	620	860	800	670	870		47	Cr
119	177	173	116	85	244	279	365	256	255	261	221	260		8	Ni
4	6	5	1	13	5	3	4	7	5	5	3	4	5	8	Rb
224	43	43	53	104	144	38	54	287	392	328	183	90	105	107	Sr
25	10	10	5	23	25	17	10	40	70	45	15	15	8	50	Ba
17	7	8	10	9	21	6	6	18	6	7	13	7	9	61	Zr
<1	2	<1	<1	1	1	<1	<1	2	1	1	<1	<1		1	Nb
10	8	8	8	8	10	8	8	10	8	8	8	7	11	26	Y
71.3	74.3	74.0	71.5	68.3	71.8	72.4	73.8	73.9	74.3	74.3	74.5	74.5	74.3	28.3	Mg No.
5.4	5.7	5.5	8.2	11.2	3.4	4.6	4.0	4.5	4.7	5.1	5.4	3.4	2.1	31.3	Q
120	197	172	150	153	109	240	260	123	230	214	129	189	153	105	Ti/Zr
II		III	III	III	II	III	III	II	III	III	?	III			Geochemical group
															Petrography
							ol	ol	ol	ol					Phenocrysts
ol			o,ol		ol*	ol	ol*	ol	o,ol,a	ol,o		ol		f,a	Micro-phenocrysts
a,o	ol*	ol	f,o,q	a,o,ol	ol*	a,ol,o	ol	ol	a	a,o	ol	ol		f,a	Groundmass: equant
a	a,ol	a,ol	a	a,o,am	a,ol	a	a	a	a	a	a	a			quench
4	2	2	4	3	2	1	3	1	4	3	3	3		5	Alteration

Phenocrysts are >1 mm
Microphenocrysts are usually between 0.3 and 0.6 mm in diameter. In some rocks, crystals of this size are skeletal (*).
Groundmass consists of small grains with normal crystal habits but predominantly of skeletal forms, set in a matrix of glass. Most samples contain 40–60% glass or its alteration products; only nos. 8 and 21 are holocrystalline.
Alteration style and its extent fall into five broad categories (see text): 1. Olivine completely unaltered, very minor replacement of glass by smectite. 2. Fresh or slightly altered olivine, significant fraction of glass replaced by smectite. 3. Significant fraction of olivine and glass altered. 4. Olivine completely altered. The extent of alteration of glass is variable. 5. Small amounts of secondary quartz are present. In all rocks, pyroxene and plagioclase are completely unaltered but vesicles are infilled by smectite, except in the case of the LPL sample which has approximately half its vesicles infilled by silica

elements are categorised into three types: compatible (Sc–Ni, Table 6), low field strength (LFS: Rb, Sc, Ba) and high field strength (HFS: Zr, Nb, Y and Ti).

Considering the compatible elements first, Cr and Ni values are high and follow MgO with a median Ni/Cr of 0.32. The Cr values agree with those of Simonian and Gass (1978) but their Ni analyses are 30–40% higher for rocks of similar MgO content. Sc and V are fairly constant over the range 8–16% MgO.

The LFS elements, including K, are the most susceptible to alteration. Rb and Ba values appear reliable but Sr is abnormally high in at least six samples. K/Rb and Rb/Sr ratios in the least altered rocks (category 1, Table 6) are 230–450 and 0.02–0.22 respectively.

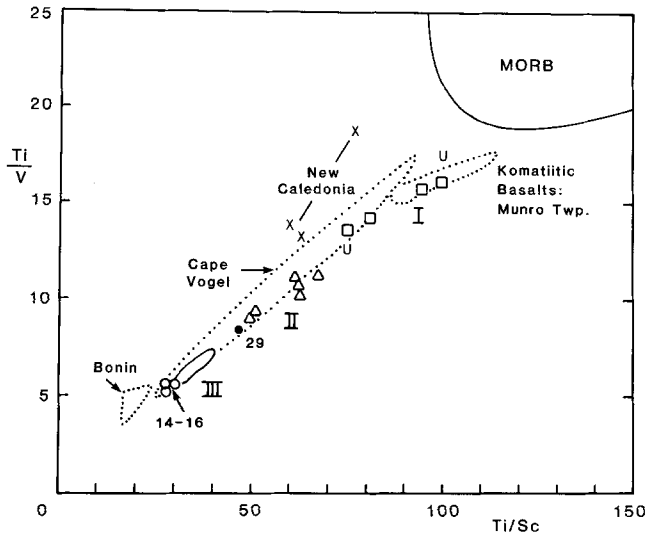

Fig. 6. Variation of Ti/V and Ti/Sc in primitive Troodos lavas. Symbols as in Fig. 5, U = samples 8 and 9. Data for boninites from Hickey and Frey (1982, Bonin Is. and MORB), D.A. Walker (unpublished, Cape Vogel). Cameron et al. (1983, New Caledonia), Arndt and Nesbitt (1982, Munro Twp.)

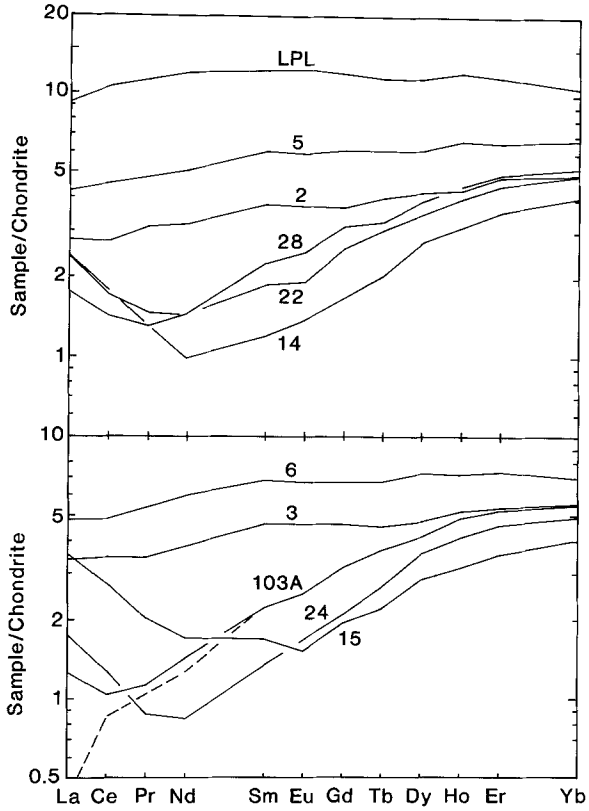

Fig. 7. Chondrite-normalised REE abundances in primitive Troodos lavas. Normalising values of Taylor and Gorton (1977). Dashed LREE profile for sample 103A from Kay and Senechal (1976)

Among the HFS elements, Zr varies from 35 to as low as 6 ppm and, like Ti, is a key element in distinguishing the three groups of lavas. Ti/Zr ratios have a huge spread, from 260 to 71. Y correlates well with Zr only for Groups I and II lavas in which Zr/Y lies between 1.7 and 2.4. Most values of Zr/Y in Group III rocks are close to 1.0. Ti/V and Ti/Sc have a large spread of values from 5.4–17.4 and 28–100 respectively (Fig. 6) mainly because of the difference in Ti content between the groups. Nb was too close to the detection limit by XRF (0.5–1 ppm) and unfortunately not free from interferences by SMSS and so is not used in later petrogenetic arguments.

Rare-earth elements

REE analyses for ten primitive rocks and the LPL sample are given in Table 7 and normalised values plotted in Fig. 7. All samples are light rare-earth element- (LREE-) depleted and none have Eu anomalies outside experimental error (±5%). Three types of patterns can be distinguished: those of Groups I and II lavas with $La_N/Yb_N \sim 0.6$, and those with U-shaped profiles, of which there are two types, slightly LREE-enriched with $Yb_N \sim 5$ (most Group III lavas) and more strongly LREE-enriched, but still with $La_N/Yb_N < 1$, and $Yb_N = 4$ (samples 14 and 15).

The results for Group III rocks contrast with published data on sample 103A (Kay and Senechal 1976) and two samples from the AFB (Simonian and Gass 1978), all of which show monotonically decreasing normalised REE abundances towards the LREE. The latter authors' third sample, no. 734, has a discontinuity in its REE profile at Nd, but unfortunately La could not be analysed, thereby preventing detection of any LREE "kick". Hints of discontinuities in the REE patterns of Desmons et al. (1980) are lost because Ce and Nd were not analysed. It is impossible to assess which geochemical group their fresh samples belong because two have REE analyses only and the third no Zr analysis. Smewing and Potts (1976) analysed two Group II samples (6aXT and 22PK) whose REE patterns are similar to nos. 2 and 3, Table 6, allowing for the fact that Ce is difficult to measure more precisely than ±10% by instrumental neutron activation (INAA) at such low levels.

There are a number of reasons why the results of this study are out of step with others: (1) interferences in LREE lines by the SSMS technique, (2) contamination during sample preparation, (3) secondary alteration effects, or (4) unreliable results from other laboratories. Interferences in ^{139}La and ^{143}Nd occur only in plagioclase-rich samples with CaAl oxides and carbides. In Ti-rich samples, interferences on ^{139}La and ^{140}Ce are known. Series of peaks at equally spaced mass numbers were looked for confirming any of the above, but not found. R.W. Kay kindly provided sample 103A which was prepared for REE analysis directly from his container. This sample was also run by INAA (B.W. Chappell, analyst) and isotope dilution (J. Foden, Adelaide University, analyst). The results unequivocally confirm the U-shaped profile and accuracy of the SSMS technique. Laboratory contamination could only be of a multielement variety, for example, physical mixing with ~1% of a granitoid (which dominate the preparation facilites) or ~0.2% of extremely LREE-enriched rocks. Splitters and mills were carefully cleaned before use and can be ruled out as sources of contamination. Given the conclusion that REE abundances have been accurately measured, there remains the possibility that they owe their LREE-enrichment to secondary processes.

Alteration

It has been argued in a previous section that with perfect textural preservation and alteration only of olivine and glass, minimal chemical modification should have occurred in the samples chosen for analysis. Conventional criteria for the freshness or otherwise of basic rocks are Fe_2O_3/FeO, H_2O^+, H_2O^- and CO_2 contents. The least altered rocks petrographically (category 1; 12 out of 30) have $Fe_2O_3/FeO < 0.38$ and as low as 0.20. Only three samples have $Fe_2O_3/FeO > 0.50$. Many rocks contain small amounts of calcite but the highest CO_2 value is 0.51 wt% corresponding approximately to only 1 modal % calcite. A 'loss on ignition' of 4–5 wt% is standard for the freshest primitive lavas, and by the criteria normally applied to basaltic rocks, these would appear to be thoroughly altered. Much of the H_2O^+ is in the glass which makes up 30–40 modal % in most samples. Unaltered glass yields microprobe totals of 93%. H_2O^- correlates with the amount of smectite, the least altered sample having values in the order of 0.5%.

There are two ways of estimating the primary H_2O^+ content of the glass: by D/H and O isotopic studies on separated material or, indirectly, by assessing the amount of seawater interaction from initial $^{87}Sr/^{86}Sr$ ratios. One sample lies within the "mantle array" on a $^{143}Nd/^{144}Nd$ (or ε_{Nd}) vs. $^{87}Sr/^{86}Sr_{(I)}$ plot (McCulloch and Cameron 1983). This is no. 2, with 3.2 wt% H_2O^+. If it is reasonable to assume that isotopic exchange of Sr and addition of H_2O^+ are coupled, 3 wt% H_2O^+ would be a maximum value in the initial magma at least for Group II lavas. This would be more than sufficient to account for the late-stage crystallisation of primary hornblende.

In the case of trace elements, Sc, V, Cr, Ni, Zr, Nb, Y and the heavy REE are considered immobile. Two sets of margin-core data confirm this and the homogeneity argument. Sr is mobile (c.f. samples 18, 26–28) and may be concentrated in a smectite. Rb and Ba appear to show a greater coherence than K although all are somewhat unreliable. A LREE kick in Group III lavas would be explained if the smectites could be shown to be LREE-enriched. There are two major difficulties with this hypothesis: the fact that there is no correlation between the degree of LREE enrichment (Fig. 7) and the modal amount of smectite via the petrographic criteria (Table 6) and the fact that sample 103A which is furtherest to the right of the mantle array (McCulloch and Cameron 1983), is the least LREE enriched.

In view of the above discussion, and in the absence of any contrary evidence, it is concluded that LREE concentrations as measured approach primary values. Lavas with distinctively different geochemical characteristics have been erupted in the same magmatic episode; the following discussion attempts to interpret this unexpected feature.

Petrogenesis

Smewing and Potts (1976), on the basis of REE patterns, first pointed out that the primitive LREE-depleted UPL required a multistage melting process if they were to be related to more fractionated lavas. They chose as a potential source a tectonised plagioclase lherzolite found in outcrop (Menzies and Allen 1974) and concluded that the equivalent of Group II lavas of this study could be derived by 12% equilibrium melting of this source, extraction of the liquid, and then a similar degree of melting of the residue. Wood (1979) extended this by means of a dynamic melting model to account for the extreme LREE-depletion thought to be present in Group III lavas (e.g. sample 103A).

Jaques and Green (1980) in anhydrous partial metling studies of the very depleted Tinaquillo lherzolite ($La_N/Yb_N \sim 0.01$) found that quartz-normative liquids could be produced only at pressures $\leqq 5$ kB. At 5 kB, 1300° C, a 21% partial melt yielded a liquid with ~14% MgO, ~51% SiO_2 and a Mg no. of 77 which, except for the SiO_2 value, closely resembles some of the more magnesian rocks of Table 6. Duncan and Green (1980) adopted the alternative approach of choosing a suitable primary liquid composition and determining the pressure and temperature at which it became saturated in olivine and orthopyroxene (harzburgite rsidue). From published major element data, they arrived at a liquid with ~52% SiO_2, ~16% MgO and a Mg no. also of 77 which, using Roeder and Emslie's (1970) K_D of 0.30, would be in equilibrium with olivine of composition $Fo_{91.8}$ (c.f. Table 1). This liquid, under anhydrous conditions, would be in equilibrium with harzburgite at 7–8 kB, 1360°. Both sets of experimental data agree on the Mg no. of the parental liquid and its silica content but Duncan and Green's estimate of pressure is more realistic geologically.

The SiO_2 content of possible parental magmas to Troodos is, however, a vital parameter. Cameron (1980) foreshadowed that a composition like that of sample 16 (Table 6, Fig. 5) would be a suitable parental magma, with 13.7% MgO and 54% SiO_2 (calculated anhydrous). Jaques and Green (1980) commented that melting under water-saturated conditions results in liquids with 6 wt% more SiO_2 than those produced at the same P, T anhydrous. A qualitative solution to the silica problem would be if $a_{H_2O} \sim 0.3$ during melting (c.f. Walker and Cameron 1982), thereby accounting for the presence of quench amphibole and hydrous glass. The tectonic repercussions of having hydrous (but not water-saturated) melting will be discussed in the following section.

U-shaped REE patterns, as found in the most primitive Troodos lavas, suggest addition of a LREE-enriched component to a LREE-depleted source region (Sun and Nesbitt 1978). This could have taken place either during the melting event or, more likely, sometime prior to melting. Such patterns are unusually common in peridotites from ophiolites (reviewed by Frey 1983) and are seen in the Troodos plagioclase lherzolite mentioned previously.

Small amounts of LREE-enrichment can be detected only in Group III lavas, either because of their very low levels of REE abundances or because the enriched component which may have affected the source of Groups I and II lavas had a much flatter REE profile. Adopting the model described in Cameron et al. (1983) whereby a single LREE-component has modified the Group III peridotite source, an estimate of $La_N/Sm_N \sim 10$ in the fluid can be made from samples 14 and 15 (Fig. 7), assuming that if its source had not been enriched, the samples would have had La_N concentrations of 0.15 and 0.20 respectively (La_N*, Table 7). Note that this ignores differences in values for distribution coefficients between La and Sm, and assumes an equilibrium melting model. The LREE profile of this component resembles those of the more LREE-enriched kimberlites with $La_N \sim 800$, $La_N/Yb_N \sim 150$ and La_N/Sm_N ratios of ~8 (McCulloch et al. 1983). The amount of enriched component required to balance La concentrations

Table 7. SSMS analyses of REE, Hf and Pb

Analysis	2	3	5	6	14	15	22	24	28	103A	103A			LPL
Field No.	201	29473	91	95	106	92	94	110	116		SSMS	ID	INAA	205
La	0.88	1.06	1.35	1.52	0.72	1.09	0.76	0.55	0.56	0.40	0.44	0.39	0.35	2.91
Ce	2.22	2.83	3.71	3.89	1.46	2.19	1.40	1.04	1.15	0.83	0.87	0.78	0.7	8.70
Pr	0.36	0.40	0.56	0.62	0.15	0.23	0.17	0.10	0.15	0.13	0.13			1.33
Nd	1.91	2.27	3.03	3.37	0.58	1.02	0.85	0.50	0.87	0.86	0.79	0.93		7.25
Sm	0.73	0.88	1.16	1.32	0.23	0.32	0.36	0.26	0.44	0.43	0.43	0.49	0.41	2.37
Eu	0.27	0.33	0.43	0.48	0.10	0.11	0.14	0.11	0.18	0.18	0.18		0.186	0.90
Gd	0.96	1.18	1.59	1.72	0.44	0.51	0.67	0.54	0.82	0.83	0.83			3.11
Tb	0.20	0.22	0.30	0.33	0.10	0.11	0.15	0.13	0.16	0.18	0.18		0.18	0.57
Dy	1.39	1.53	1.99	2.35	0.90	0.93	1.15	1.15	1.28	1.34	1.34	1.50		3.79
Ho	0.32	0.37	0.49	0.52	0.23	0.23	0.30	0.31	0.33	0.35	0.35		0.34	0.90
Er	1.03	1.10	1.40	1.57	0.76	0.75	0.97	1.00	1.02	1.10	1.10	1.14		2.51
Yb	1.04	1.14	1.41	1.46	0.84	0.84	1.04	1.06	1.11	1.20	1.20	1.22	1.11	2.19
Hf	0.7	0.6	0.9	0.9	0.2	0.3	0.3	0.2	0.3	0.4				1.3
Pb	1.07	1.04	1.10	0.87	1.54	2.77	2.66	0.83	1.27	0.55				0.66
La_N/Yb_N	0.56	0.61	0.63	0.69	0.57	0.86	0.48	0.34	0.33	0.22				0.88
La^*_N					0.15	0.20	0.50	0.30	0.60	0.60				
La^*_N/Yb_N					0.04	0.05	0.10	0.06	0.11	0.11				
% added component+					0.27	0.41	0.17	0.16	0.15	0.09				

La* = Probable La concentration in sample had the source not been LREE-enriched.
+ = Relative amounts of LREE-enriched component, assuming La_N for this component is 800.
Normalisation values are Leedy chondrite ÷1.20 (La = 0.315, Yb = 0.208; see Taylor and Gorton 1977)

for Group III lavas (Table 7) is extremely small. Although the actual numbers are model-dependent and somewhat arbitrary, their relative proportions should be accurate.

In Fig. 8 ε_{Nd} is plotted against the proportion of LREE-enriched component and suggests an unmodified mantle source with ε_{Nd} between +9 and +11, characteristic of MORB sources. If the enriched component which affected Group III lavas had an ε_{Nd} of −15 (McCulloch et al. 1983), mixing could produce a spectrum of ε_{Nd} values in the modified sources, e.g. from +8 (source for sample 103A) to −2 (the plagioclase lherzolite). An intermediate extent of enrichment, as proposed for samples 24 and 28 (Table 7) would satisfy the ε_{Nd} value of the Group II lavas (~ +5, McCulloch and Cameron 1983) but is not obvious from their REE patterns. The preferred solution is to assume that the second component in this case had REE characteristics like those deduced for Tertiary (low-Ca boninites) with La_N/Sm_N ~2.5 and a less negative ε_{Nd} value (Cameron et al. 1983).

The ideas expressed above have been derived from REE and isotopic data alone. Since there is five times as much as La in the most enriched Group III lava (no. 15) than the value estimated by extrapolation of the monotonically decreasing part of its REE profile (La*, Table 7), similar effects should be seen in elements with similar degrees of incompatibility: the LFS elements including K and Pb, and to a lesser extent the HFS elements P and Zr. A strong correlation exists for Zr (Fig. 8) and less convincing ones for Rb, Ba, Pb and K. Aberrant results such as Ba in sample 28 and Pb and K in no. 22 can be ascribed to alteration, as have many of the Sr analyses. Unfortunately, data for Nb, Hf and P are not sufficiently precise to use.

Having established geochemical and isotopic regularities within Group III lavas and noted the role of olivine fractionation within Group I and II lavas (Fig. 5), it remains to explore the relationships between Groups I, II and III lavas. Compatible elements, such as Ni, Cr, Sc and V do not vary markedly between rocks of similar MgO content in different groups whereas significant differences exist in their TiO_2, Na_2O, Zr and REE abundances (Figs. 5, 7). The clustering into three groups with decreasing HFS element contents is best shown on a Ti−Zr plot (Fig. 9). Samples 14–16, while having the major element characteristics of Group III lavas are unusually enriched in Zr and, for the purposes of the following discussion, are henceforth termed IIIa. Group I lavas have chondritic Ti/Zr ratios but are more depleted in the HFS elements than MORB (Table 8) as are komatiitic basalts. Group II lavas have lower Ti and Zr (only slightly higher Ti/Zr ratios) and REE profiles parallel to those of Group I. Group III lavas are further depleted in LFS and HFS elements but not HREE and have an average Ti/Zr of 200. Group IIIa lavas have lower HREE but are significantly enriched in LFS elements as well as Zr and trend toward the low Ti/Zr ratios which characterise Tertiary boninites. Many of the commonly quoted ratios in Table 8 involve Ti which is one of the main causes of the differences between groups.

Groups I, II and III cannot be related by crystal fractionation since olivine, orthopyroxene and clinopyroxene phenocrysts all have extremely low concentrations of incompatible elements (Tables 1–3). The potential effect of fractionation can be seen in the ultramafic lavas (samples 8 and 9) which plot near Group III in Fig. 9. Subtraction of ~60% Fo_{91} is needed to yield MgO contents commensurate with those of the primitive lavas discussed in this paper. Calculated Ti and Zr contents consign them to Group I. To explain the differences between the groups, at least three distinct source regions are required. Sample 29 (Fig. 9) points to the possibility of limited magma mixing.

An incremental melting scheme giving rise to the three lava groupings can be modelled with REE concentrations using a depleted initial source similar to that of Smewing

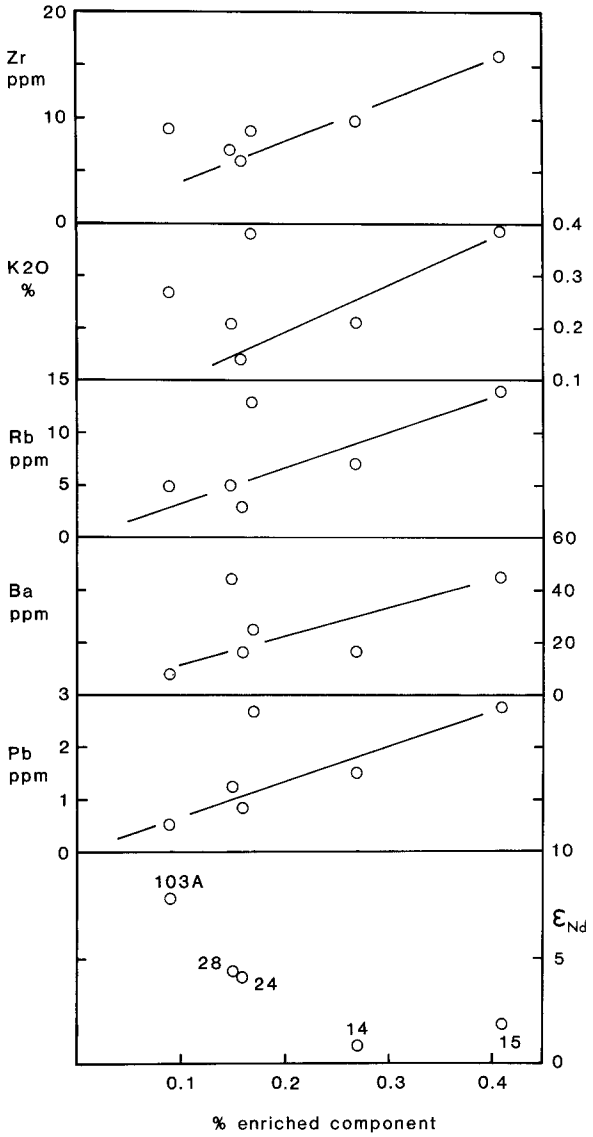

Fig. 8. Variation of certain incompatible elements and ε_{Nd} in Group III lavas with estimated proportion of enriched component present in source. Actual percentages are for the case when La_N in the enriched component = 800 and $La_N/Sm_N \sim 10$

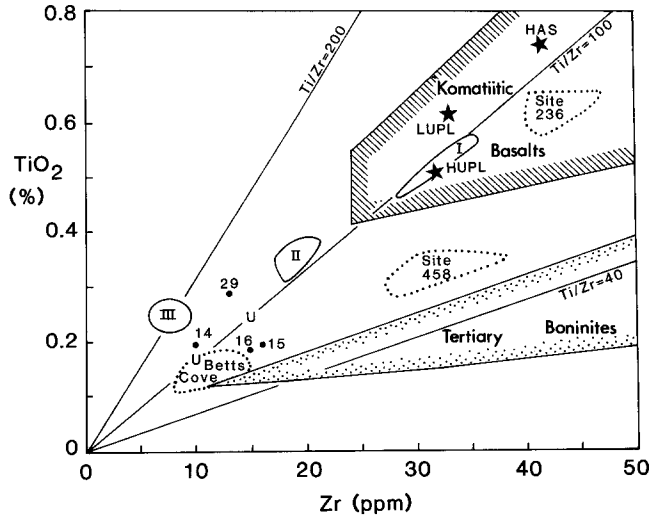

Fig. 9. Variation of Ti with Zr in primitive Troodos lavas (Groups I, II, III and samples 8, 9, 14–16 and 29) compared with that in Tertiary and Betts Cove and Site 458 boninites, komatiitic basalts and "MORB" from Site 236. Primitive MORB (Sun et al. 1979) plots in the top right corner of the diagram. *HAS* = Troodos Higher Axis sequence (LPL) average, *LUPL* = Lower UPL average, *HUPL* = Higher UPL average, all after Smewing et al. (1975). Data for komatiitic basalts from Arndt and Nesbitt (1982), E.G. Nisbet (unpublished data) and this work; for Tertiary boninites from Cameron et al. (1983) and Hickey and Frey (1982); for Betts Cove, selected data from Coish et al. (1982); Site 458 from Meijer (1980) Hickey and Frey (1982) and Wood et al. (1980); Site 236 from Frey et al. (1980)

and Potts (1976) with $La_N/Yb_N = 0.5$ and $La_N = 0.5$ but must take account of the variation in $^{143}Nd/^{144}Nd$ ratios (Table 7). Assuming the original mantle segment had the characteristics of depleted MORB ($\varepsilon_{Nd} \sim 10$), a 20–25% equilibrium partial melt of this source modified by ~0.1–0.2% of a component with $\varepsilon_{Nd} \sim -15$ could produce the spectrum of Group III lavas. Group IIIa lavas with lower HREE contents may represent <5% melts of the residue from this event with a much higher proportion of enriched component (Table 7). An even greater enrichment would give rise to boninite-like REE patterns in the lavas with

Table 8. Chemical and isotopic data for primitive Troodos lavas compared with those of MORB and boninites

	Primitive MORB	Troodos				Tertiary Boninites
		I	II	III	IIIa	
TiO_2	>0.7%	0.45–0.6%	0.30–0.40%	0.20–0.30%	0.20%	0.1–0.5%
Zr	>35 ppm	28–35 ppm	17–21 ppm	<10 ppm	10–16 ppm	10–80 ppm
Ti/Zr	~110	~100	100–120	150–260	70–115	<70
Zr/Y	2.5	2.2	2.0	1.0	2.2	3–9
Ti/V	>19	13–17	9–11	6–7	5.5	4–19
Ti/Sc	>100	75–100	50–70	30–40	28	15–90
Na_2O	>2%	1.7–2.0%	1.3–1.6%	0.7–1.2%		1–2.8%
CaO/Al_2O_3	~0.8	~0.7	0.70–0.80	0.81–0.90	0.78–0.85	<0.7
Yb_N	10	7	5	5	4	2–6
La_N/Yb_N	0.2–0.6	0.6	0.6	<0.5	0.6–0.9	1–5
ε_{Nd}	8–12	7	4–6	4–8	<2	0–8

Data for primitive MORB from Sun et al. (1979) and for Tertiary boninites from Jenner (1981), Hickey and Frey (1982), McCulloch and Cameron (1983) and Cameron et al. (1983)

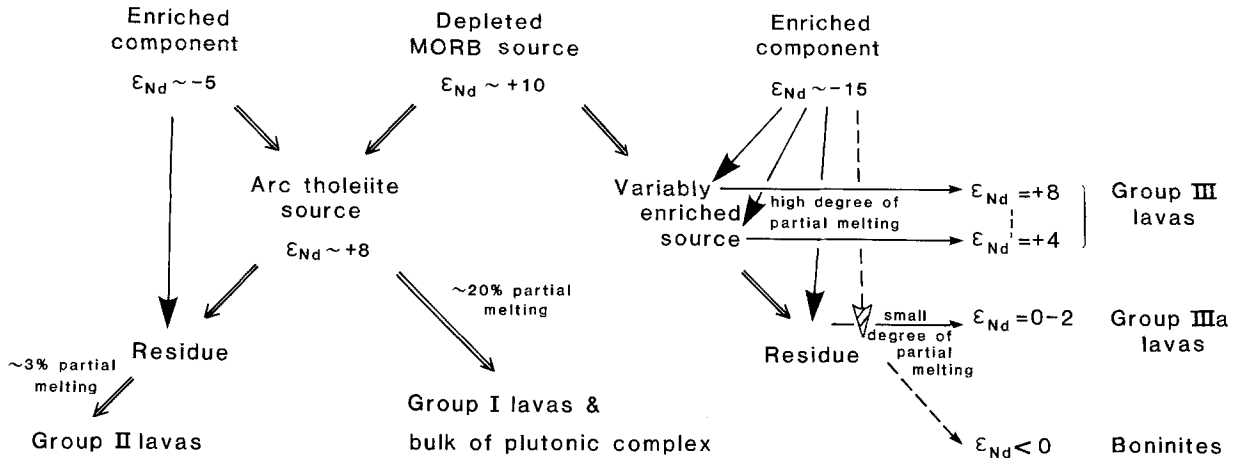

Fig. 10. Petrogenetic scheme for the Troodos ophiolite, based on the geochemistry of primitive lavas and Nd isotopic study of McCulloch and Cameron (1983). If the plagioclase lherzolite, mentioned in the text (residue in the figure) were partially melted, it would produce low-Ca boninites

$La_N/Yb_N > 1$ and negative ε_{Nd} values but only the possible peridotite source for these is seen in Cyprus.

The single Group I lava analysed for $^{143}Nd/^{144}Nd$ has a value similar to that for the LPL, to a gabbro (Richard and Allègre 1980) and to an ultramafic cumulate (McCulloch and Cameron 1983). This suggests that a liquid more magnesian than sample 6 and in equilibrium with $Fo_{91.5}$ would be a reasonable parental magma for the Troodos plutonic complex. From Fig. 5 and Roeder and Emslie's (1970) K_D of 0.30, it would have SiO_2 ~54%, MgO ~14%, $Na_2O + K_2O$ ~1.8%, TiO_2 ~0.4%, Zr ~25 ppm and La_N/Yb_N ~0.6. The order of crystallisation in Group I lavas is best seen in sample 8: ol → cpx → opx → plag which corresponds exactly to the texture in the ultramafic cumulate. The source region for Group I lavas could be derived from a depleted MORB-like one (Sun et al. 1979) by addition of an enriched component of unknown chemistry. The fact that REE abundances of Group II lavas are lower and subparallel to those of Group I suggests a higher degree of melting of the same source, but this is ruled out by Nd isotope data. In order to reduce ε_{Nd} from 8 to 4–5, a second enriched component with ε_{Nd} ~ −5 has to be added. A solution is outlined in Fig. 10 whereby the residue from melting giving rise to Group I lavas interacts further with the same or similar enriched component and undergoes a further few percent partial melting. These Group II melts appear in the plutonic complex ($\varepsilon_{Nd} = 3.8$, Hannah and Futa 1982) but their extent is not known.

An explanation of the behaviour of the non-REE trace elements relies on their degree of incompatibility. Increasing degrees of melting of a single source should lead to an increasing Ti/Zr ratio in the liquid (Pearce and Norry 1979). The high degree of melting reached in Group III lavas results in Ti/Zr ratios as high as 260, which becomes lower only when appreciable amounts of the enriched component have either added Zr relative to Ti, or a refractory Ti-rich mineral has crystallised in the source region. In Fig. 6 Sc–V–Ti behaviour can be rationalised in terms of the incompatibility of Ti relative to Sc and V. Ba_N follows the LREE trends of Fig. 6 when the patterns are extrapolated to the left of La, but K, Rb and Pb results are more scattered.

An alternative to progressive melting would be reaction between the LREE-enriched fluid and depleted peridotite, giving rise to the crystallisation of new minerals. The extremely high La_N/Sm_N ratio deduced for the Troodos enriched component can be matched only in kimberlitic rocks. Metasomatised mantle nodules in kimberlites tend to be harzburgites or depleted lherzolites which contain diopside and the hydrous minerals K-rich richterite and phlogopite and often apatite and a Ti-oxide, ilmenite or rutile (Kramers et al. 1983). Highly incompatible-enriched fluids would be expected to rise in the mantle, affecting spinel peridotites (e.g. Menzies 1983) and the even higher level source region inferred for Troodos. The chemical transition from Group I to II and within Group III might be explained by an increased extent of interaction between the enriched components and original MORB source (Fig. 10), resulting in the crystallisation of a number of incompatible element-enriched minerals in differing proportions. Although the extent of interaction is small, no sign of alkaline vulcanism which should result from small degrees of partial melting of the enriched source is seen on Cyprus. It is more likely that the sources of these components control their chemistry, for example by retaining Ti.

Petrologic and tectonic affinities

From Fig. 5 of this paper and Fig. 1 of Robinson et al. (1983), Harker diagrams covering the range 16–1% MgO can be constructed for the entire volcanic series on Troodos. There is a distinct break only in TiO_2 content at 3.8% MgO, but this may reflect a sampling problem. The higher Mg "basaltic andesite" trend of Robinson et al. begins with a parental liquid with ~14% MgO and chromite and olivine on the liquidus, followed by orthopyroxene or clinopyroxene, maintaining a steady increase in Al_2O_3 content but only a slight one in SiO_2. Plagioclase did not appear on the liquidus until an MgO value of 6% was reached, followed by Fe–Ti spinel at ~4% MgO. The late crystallisation of titanomagnetite confirms a tholeiitic trend (c.f. Irvine and Baragar 1971) but an unusual one because of the initially high SiO_2 and low Al_2O_3 contents of the liquid.

There are major mineralogical, chemical and isotopic differences between Troodos lavas and MORB (Cameron 1980, Robinson et al. 1983, McCulloch and Cameron 1983). Only altered rocks from site 256 in the Somali Basin (Frey et al. 1980) are in any way comparable to Troodos lavas. They have anomalously low Ti contents and Ti/Zr ratios

(Fig. 9) but at the same MgO values, have 2% less SiO_2 than Group I UPL and $<0.5\%$ H_2O. The association of "Cyprus-type" massive sulphide deposits with mid-ocean ridges may be fortuitous. The origin of the sulphides in the LPL may be a reflection of the fact that the host rocks are high-Si andesites or dacites which have reached S-saturation through differentiation rather than from relatively high (~ 100 ppm) concentrations in MORB-like parental liquids.

Nd isotopes (McCulloch and Cameron 1983) and LFS and HFS element concentrations point to affinities with island-arc tholeiites for the Troodos lavas, as first suggested for the LPL by Pearce (1975). The "calcalkaline" trend of Miyashiro (1973) is misleading, in fact the more differentiated rocks are tholeiites on his discriminant plots. Ti–V (Shervais 1982), Ti–Zr and Ti–Cr (Pearce 1975) and Ti–Cr–Ni diagrams (Beccaluva et al. 1979) also suggest island-arc affinities, as distinct from MORB. Neither boninites nor rocks similar to those described here have been found in island arcs. Although arc lava compositions are often complicated by the abundance of phenocrysts in them, they appear to have higher Al_2O_3 and parental magmas which are basaltic, with 3–4% less SiO_2 at an appropriate MgO level compared with Troodos UPL. The origin of H_2O and the enriched components for high-Mg, low-Ti vulcanism (e.g. Troodos) nevertheless is easiest explained by fluids arising from a subducting or previously subducted slab containing some continental-derived material.

The boninitic affinity of the Group III lavas is an important clue to tectonic setting. There is only one locality where boninites occur in a definitely established tectonic environment: the Mariana fore-arc which Cameron et al. (1979), Natland and Tarney (1980) and Bloomer (1983) have interpreted as an *in situ* ophiolite. Dredging by the last author has revealed significant amounts of orthopyroxene-bearing gabbros and serpentinised harzburgites which, along with boninite series rocks, are the key constituents of low-Ti ophiolites. Abundant serpentinised harzburgite suggests ease of obduction (and therefore preservation as a conventional ophiolite) of the fore-arc region which, notably, is thoroughly atypical of oceanic crust as a whole.

The appearance of boninites is rare and sporadic in the geological record an implies they may be triggered by unusual tectonic events. The eruption of Late Eocene boninites in the Western Pacific (including those of the Bonin Islands, Tsunawaka 1983) could have resulted from the drastic change in direction of motion of the Pacific plate 42 to 44 Ma ago (Clague and Jarrard 1973), resulting in the initiation of subduction. The heat source is a problem for shallow depths of magma generation but might be explained by stress heating in a young and relatively hot mantle wedge. Coish et al. (1982) suggested that boninites form initial back-arc, rather than fore-arc basin crust and Crawford et al. (1981) postulated that they are erupted as a consequence of splitting arcs. Both hypotheses explain difficulties relating to the heat source and tensional environment but there are no known examples. Although low Ti-ophiolites may be found in fore-arc settings, it is by no means proved that they represent fore-arc vulcanism.

Conclusions

The primitive UPL and AFB lavas comprise three main types of melt which differ subtly in their chemistry and isotopic composition. The least depleted in LFS and HFS elements (Group I) are parental to the plutonic complex and LPL. A suitable primary magma for low-Ti ophiolites like Troodos would have $\sim 54\%$ SiO_2, $\sim 14\%$ MgO, $\sim 1.8\%$ Na_2O+K_2O and $\sim 0.4\%$ TiO_2 and trace element contents remarkably similar to those of komatiitic basalts.

The other lava groups of Troodos, which are volumetrically less significant, are compositionally and isotopically diverse and require a mechanism for decoupling the HFS from other incompatible elements, which typify boninites. All were probably formed in a subducted-related environment but there is no independent evidence favouring a fore-arc setting over initial back-arc vulcanism.

Acknowledgments. This project arose from papers presented by C.R. Allen, J.A. Pearce, K.O. Simonian and J.D. Smewing at a conference at the Open University in 1975. I thank them for later discussions and S-S. Sun, M.T. McCulloch, L. Jaques, R.A. Binns and an anonymous reviewer who made helpful comments on the manuscript. B.W. Chappell and S.R. Taylor provided excellent analytical facilities and R.S. Freeman, E. Webber, J. Wasik and P. Oswald-Sealy technical assistance.

Appendix: *Nomenclature*

Finding appropriate names for the primitive Troodos lavas is not straightforward. "Low-Ti ophiolitic basalts" and "magnesian quartz-tholeiites" (Sun and Nesbitt 1978) fail to emphasise the fact that these rocks are andesitic when recast volatile-free. "High-Mg andesites" (Sun and Nesbitt 1978) may be suitable and terms "komatiitic basalt" (Simonian and Gass 1978) and "boninite" (Cameron et al. 1979) also have their place. Chemical parameters for Group I lavas lie within the range of those of komatiitic basalts (Table 8). There is one major difference: komatiitic basalts with the high SiO_2 contents typical of Group I lavas have lower Ti/Zr ratios (Fig. 9, E.G. Nisbet, unpublished data). Natland (1980, p. 698) proposed that rocks belonging to the boninite series should be recognised by order of crystallisation of their minerals: low-Ca pyroxene$\pm$olivine, augite, plagioclase. On this basis the orthopyroxene-bearing primitive UPL and AFB rocks of Groups II, III and IIIa would be boninites whereas those of identical chemistry but without low-Ca pyroxene would not, a problem which Cameron et al. (1979) attempted unsuccessfully, to solve. Perhaps the broader term boninitic "affinity" will suffice.

References

Adamides NG (1980) The form and environment of formation of the Kalavasos ore deposits – Cyprus. In: A Panayiotou (ed) Ophiolites. Geol Surv Dept, Nicosia, pp 117–128

Arndt NT, Fleet ME (1979) Stable and metastable pyroxene crystallization in layered komatiite lava flows. Am Mineral 64:856–864

Arndt NT, Nesbitt RW (1982) Geochemistry of Munro Township basalts. In: Arndt NT, Nisbet EG (eds) Komatiites. Allen and Unwin, London, pp 309–329

Bear LM (1960) The geology and mineral resources of the Akaki-Lythrondha area. Mem Geol Surv Cyprus 3:1–122

Beccaluva L, Ohnenstetter D, Ohnenstetter M (1979) Geochemical discrimination between ocean floor and island arc tholeiites. Application to some ophiolites. Ofioliti 4:67–72

Bloomer SH (1983) Distribution and origin of igneous rocks from the landward slopes of the Mariana Trench: implication for its structure and evolution. J Geophys Res 88:7411–7428

Cameron WE (1980) Comment on 'Role of multistage melting in the formation of oceanic crust' by Duncan RA, Green DH. Geology 8:562

Cameron WE, Nisbet EG (1982) Phanerozoic analogues of koma-

tiitic basalts. In: Arndt NT, Nisbet EG (eds) Komatiites. Allen and Unwin, London, pp 29–50
Cameron WE, Nisbet EG, Dietrich VJ (1979) Boninites, komatiites and ophiolitic basalts. Nature 280:550–553
Cameron WE, Nisbet EG, Dietrich VJ (1980) Petrographic dissimilarities between ophiolitic and ocean-floor basalts. In: Panayiotou A (ed) Ophiolites. Geol Surv Dept, Nicosia,, pp 182–192
Cameron WE, McCulloch MT, Walker DA (1983) Boninite petrogenesis: chemical and Nd–Sr isotopic constraints. Earth Planet Sci Lett 65:75–89
Clague DA, Jarrard RD (1973) Tertiary Pacific plate motion deduced from the Hawaiian-Emperor chain. Bull Geol Soc Am 84:1135–1154
Coish RA, Hickey R, Frey FA (1982) Rare earth element geochemistry of the Betts Cove ophiolite. Newfoundland: complexities in ophiolite formation. Geochim Cosmochim Acta 46:2117–2134
Coleman RG (1977) Ophiolites. Springer-Verlag, Berlin, 299 pp
Crawford AJ, Beccaluva L, Serri G (1981) Tectono-magmatic evolution of the West Philippine-Mariana region and the origin of boninites. Earth Planet Sci Lett 54:346–356
Desmet A (1976) Evidence of co-genesis of the Troodos lavas, Cyprus. Geol Mag 113:165–168
Desmet A, Lapierre H, Rocci G, Gagny Cl, Parrot J-F, Delaloye M (1978) Constitution and significance of the Troodos sheeted complex. Nature 273:527–530
Desmons J, Delaloye M, Desmet A, Gagny Cl, Rocci G, Voldet P (1980) Trace and rare earth element abundances in Troodos lavas and sheeted dykes, Cyprus. Ofioliti 5:35–56
Dick HJB, Bullen T (1984) Chromian spinel as a petrogenetic indicator in oceanic environments. Contrib Mineral Petrol 86:54–76
Donaldson CH (1976) An experimental investigation of olivine morphology. Contrib Mineral Petrol 57:187–213
Duncan RA, Green DH (1980) Role of multistage melting in the formation of oceanic crust. Geology 8:22–26
Fleet ME (1975) Growth habits of clinopyroxene. Can Mineral 13:336–341
Frey FA (1983) Rare earth element abundances in upper mantle rocks. In: Henderson P (ed) Rare earth element geochemistry, Elsevier, Amsterdam
Frey FA, Dickey JS Jr, Thompson G, Bryan WB, Davies HL (1980) Evidence for heterogeneous primary MORB and mantle sources, NW Indian Ocean. Contrib Mineral Petrol 74:387–402
Gass IG (1958) Ultrabasic pillow lavas from Cyprus. Geol Mag 95:241–251
Gass IG, Smewing JD (1973) Intrusion, extrusion and metamorphism at constructive margins: evidence from the Troodos Massif, Cyprus. Nature 242:26–29
Greenbaum D (1972) Magmatic processes at ocean ridges: evidence from the Troodos Massif, Cyprus. Nature Phys Sci 238:18–21
Greenbaum D (1977) The chromitiferous rocks of the Troodos ophiolite complex, Cyprus. Econ Geol 72:1175–1194
Hannah JL, Futa K (1982) Nd, Sr and O isotope systematics in the Troodos ophiolite, Cyprus. Geol Soc Am Absts 14:506
Hickey RL, Frey FA (1982) Geochemical characteristics of boninite series volcanics: implications for their source. Geochim Cosmochim Acta 46:2099–2115
Irvine TN, Baragar WRA (1971) A guide to the chemical classification of the common volcanic rocks. Can J Earth Sci 8:523–548
Jaques AL, Green DH (1980) Anhydrous melting of peridotite at 0–15 Kb pressure and the genesis of tholeiitic basalts. Contrib Mineral Petrol 73:287–310
Jaques AL, Chappell BW, Taylor SR (1983) Geochemistry of cumulus peridotites and gabbros from the Marum Ophiolite Complex, northern Papua New Guinea. Contrib Mineral Petrol 82:154–164
Jenner GA (1981) Geochemistry of high-Mg andesites from Cape Vogel, Papua New Guinea. Chem Geol 33:307–332
Jørgensen KA, Brooks CK (1981) The Troodos ophiolite: petrology of a fresh glassy basalt. Bull Geol Soc Denmark 30:43–50
Kay RW, Senechal RG (1976) The rare earth geochemistry of the Troodos ophiolite complex. J Geophys Res 81:964–970
Kramers JD, Roddick JCM, Dawson JB (1983) Trace element and isotope studies on veined, metasomatic and "MARID" xenoliths from Bultfontein, South Africa. Earth Planet Sci Lett 65:90–106
Lapierre H (1972) Geological map of the Polis-Paphos area. Geol Surv Dept, Nicosia
Lapierre H, Rocci G (1976) Le volcanism alkalin du sud-ouest de Chypre et le problème de l'ouverture des régions Tethysiennes au Trias. Tectonphys 30:299–313
McCulloch MT, Cameron WE (1983) Nd–Sr isotopic study of primitive lavas from the Troodos ophiolite, Cyprus: evidence for a subduction-related setting. Geology 11:727–731
McCulloch MT, Jaques AL, Nelson DR, Lewis JD (1983) Nd and Sr isotopes in kimberlites and lamproites from Western Australia: an enriched mantle origin. Nature 302:400–403
Meijer A (1980) Primitive arc vulcanism and a boninite series: examples from western Pacific island arcs. In: Hayes DE (ed) The tectonic and geologic evolution of southeast Asian seas and islands. Am Geophys Union Monogr 23:269–282
Menzies MA (1983) Mantle ultramafic xenoliths in alkaline magmas: evidence for mantle heterogeneity modified by magmatic activity. In: Hawkesworth CJ, Norry MJ (eds) Continental basalts and mantle xenoliths, Shiva Press, London, pp 92–110
Menzies MA, Allen CR (1974) Plagioclase lherzolite – residual mantle relationships within two eastern Mediterranean ophiolites. Contrib Mineral Petrol 45:197–213
Miyashiro A (1973) The Troodos ophiolitic complex was probably formed in an island arc. Earth Planet Sci Lett 19:218–224
Moores EM, Vine FJ (1971) The Troodos Massif, Cyprus and other ophiolites as oceanic crust: evaluation and implications. Phil Trans R S London, Ser A 268:443–466
Natland JH (1980) Crystal morphologies and pyroxene compositions in boninites and tholeiitic basalts from DSDP Holes 458 and 459B in the Mariana fore-arc region. In: Hussong DM, Uyeda S et al. (eds) Init Repts DSDP 60, US Govt Ptg Office, Washington, pp 681–707
Natland JH, Tarney J (1980) Petrologic evolution of the Mariana arc and back-arc basin system – a synthesis of drilling results in the South Philippine Sea. In: Hussong DM, Uyeda S et al. (eds) Init Repts DSDP 60, US Govt Ptg Office, Washington, pp 877–908
Norrish K, Chappell BW (1977) X-ray fluorescence spectrometry. In: Zussman J (ed) Physical methods in determinative mineralogy. Academic Press, London, pp 201–272
Pantazis Th M (1967) The geology and mineral resources of the Pharmakas-Kalavasos area. Cyprus Geol Surv Mem 8
Pantazis Th M (1969) 1:250000 geological map of Cyprus. Geol Survey Dept, Nicosia
Pearce JA (1975) Basalt geochemistry used to investigate past tectonic environments on Cyprus. Tectonophys 25:41–67
Pearce JA, Norry MJ (1979) Petrogenetic implications of Ti, Zr, Y and Nb variations in volcanic rocks. Contrib Mineral Petrol 69:33–47
Richard P, Allègre CJ (1980) Neodymium and strontium isotope study of ophiolite and orogenic lherzolite petrogenesis. Earth Planet Sci Lett 47:65–74
Robinson PT, Melson WG, O'Hearn T, Schmincke H-U (1983) Volcanic glass compositions of the Troodos ophiolite, Cyprus. Geology 11:400–404
Roeder PL, Emslie RF (1970) Olivine-liquid equilibrium. Contrib Mineral Petrol 29:275–289
Searle DL, Vokes FM (1969) Layered ultrabasic lavas from Cyprus. Geol Mag 106:515–530
Serri G (1981) The petrochemistry of ophiolite gabbroic complexes: a key for the classification of ophiolites into low-Ti and high-Ti types. Earth Planet Sci Lett 52:203–212
Shervais JW (1982) Ti-V plots and the petrogenesis of modern and ophiolitic lavas. Earth Planet Sci Lett 59:101–118

Simonian KO, Gass IG (1978) Arakapas fault belt, Cyprus: a fossil transform fault. Geol Soc Am Bull 89:1220–1230

Smewing JD, Potts PJ (1976) Rare-earth abundances in basalts and metabasalts from the Troodos Massif, Cyprus. Contrib Mineral Petrol 57:245–258

Smewing JD, Simonian KO, Gass IG (1975) Metabasalts from the Troodos Massif, Cyprus: genetic implication deduced from petrography and trace element geochemistry. Contrib Mineral Petrol 51:49–64

Swarbrick RE (1980) The Mamonia complex of SW Cyprus: a Mesozoic continental margin and its relationship to the Troodos complex. In: Panayiotou A (ed) Ophiolites. Geol Surv Dept, Nicosia

Sun S-S, Nesbitt RW (1978) Geochemical regularities and genetic significance of ophiolitic basalts. Geology 6:689–693

Sun S-S, Nesbitt RW, Sharaskin A Ya (1979) Geochemical characteristics of mid-ocean ridge basalts. Earth Planet Sci Lett 44:119–138

Taylor SR, Gorton MP (1977) Geochemical application of spark source mass spectrography – III. Element sensitivity, precision and accuracy. Geochim Cosmochim Acta 41:1375–1380

Tsunakawa H (1983) K – Ar dating on volcanic rocks in the Bonin Islands and its tectonic implication. Tectonophys 95:221–232

Walker DA, Cameron WE (1983) Boninite primary magmas: evidence from the Cape Vogel Peninsula, PNG. Contrib Mineral Petrol 83:150–158

Wood DA (1979) Dynamic partial melting: its application to the petrogenesis of basalts erupted in Iceland, the Faeroe Islands, the Isle of Skye (Scotland) and the Troodos Massif (Cyprus). Geochim Cosmochim Acta 43:1031–1046

Wood DA, Marsh NG, Tarney J, Joron J-L, Fryer P, Treuil M (1980) Geochemistry of igneous rocks recovered from a transect across the Mariana Trough, arc, fore-arc, and trench, Sites 453 through 461, DSDP Leg 60. In: Hussong DM, Uyeda S et al. (eds) Init Repts DSDP 60, US Govt Ptg Office, Washington, pp 611–645

Received April 17, 1984 / Accepted October 25, 1984